Pulse Flow Enhancement in Two-Phase Media

by

Robert P. Zschuppe

A thesis
presented to the University of Waterloo
in fulfillment of the
thesis requirement for the degree of
Master of Science
in
Earth Science

Waterloo, Ontario, Canada, 2001

I hereby declare that I am the sole author of this thesis. This is a true copy of the thesis, including any required final revisions, as accepted by my examiners.

I understand that my thesis may be made electronically available to the public.

Acknowledgements

There are many people who provided advice and help during my studies that I would like to thank. First, the people that assisted construction of the Consistent Pulsing Source (CPS): Ke Xian Au Yong, Len Tober, and Brett Davidson. Secondly, Steve Gamble and Dr. Rick Chalaturnyk for providing pressure transducers, a lab computer, and for helping install the monitoring equipment. Dr. Tim Spanos for his equipment, time, and extremely valuable insight into porous media physics. For helping me out with the labs, which could often be quite strenuous, Ke Xian Au Yong, Jinsong Wang, Xiaowei Lui, Marko Mah, and Darrell Shand. And finally, to those that provided direction during my studies: Dr. Maurice Dusseault, Dr. Rick Chalaturnyk, and Dr. Tim Spanos.

I would also like to thank Subterranean Technologies Incorporated (STI) and the National Sciences and Engineering Research Council of Canada (NSERC) for their financial support during these studies.

Abstract

This laboratory project has been done to evaluate pressure pulsing as an Enhanced Oil Recovery (EOR) technique. To perform the study, a consistent laboratory methodology was developed, including the construction of a Consistent Pulsing Source (CPS). Tests compared pulsed and non-pulsed waterfloods in a paraffin or crude oil saturated medium, which also contained connate water (an irreducible water saturation). Results revealed that pulsed tests had maximum flow rates 2.5–3 times higher, greater oil recovery rates, and final sweep efficiencies that were more than 10% greater than non-pulsed tests.

The CPS design has proven very successful, and has since been copied by a major oil corporation. However, there are two limitations, both caused by fluctuating water reservoir levels. Longer pulsed tests (reservoir-depletion tests) were periodically paused to refill the water reservoir, resulting in reservoir depressurization and lower flow rates. The final effect of this was impossible to quantify without correcting the problem. The second CPS limitation was the change in pulse shape with time. However, it is not expected that this had any major effect on the results.

The pulse pressure and period studies were limited by early tests, which did not have the necessary time duration. Both increasing pulse pressure and decreasing pulse period were found to increase the final sweep efficiency.

Slightly decreasing porosity (0.4% lower) was found to lower sweep efficiencies. However, the 34.9% porosity results were not done until reservoir depletion, so it is difficult to quantitatively compare results.

An emulsion appeared after water breakthrough when using the CPS on light oils (mineral oil). This may have been the result of isolated oil ganglia being torn apart by the sharp pulses.

Although it is difficult to apply laboratory results to the field, this study indicates that pressure pulsing as an EOR technique would be beneficial. Doubled or tripled oil recovery rates and 10% more oil recovery than waterflooding would be significant numbers in a field operation. A valuable application would be in pulsing excitation wells to both pressurize the reservoir and enhance the conformance of the displacing fluid over a long-term period. It would also be valuable for short-term chemical injections, where mixing with the largest volume possible is desirable.

Contents

List of Tables

List of Figures

Chapter 1

Introduction

Pressure pulsing is a new enhanced oil recovery and contaminant cleanup technique used in both the petroleum and environmental industries. Laboratory tests were first started in January 1997, the first full-scale oil reservoir field-test in December 1998, and the first environmental field-test in June 2000. Because of pulsing's short history, there is still much to be learned about its advantages and limitations; and the easiest way to learn is in the lab.

Prior experimental work focused on single-fluid systems or was largely demonstrative and used to verify underlying physical theory. The next step is to quantify the effects of pulsing in a two-phase system (water displacing oil); a step which necessitates development of new lab equipment and methodologies to ensure meaningful results. Naturally, any information and experience gained with pulsing in the laboratory will be very useful in the field.

1.1 Project Objectives

- Develop a consistent testing methodology, including the construction of the Consistent Pulsing Source (CPS).
- Compare the sweep efficiencies, oil recovery rates, and flow rates, of selected pulsed and non-pulsed tests.
- Analyze or observe the effect of pulse pressure, pulse period, and porosity on the sweep efficiencies of pulsed tests.
- Observe the test conditions under which an emulsion is formed.

In the field, the pulse period/pulse pressure studies are very important. For example, in the heavy oil industry, pulsing is carried out using a plunger-type attachment at the end of a tubing or rod string. This "plunger" is raised and lowered in the wellbore, creating pressure pulses in

the reservoir. The distance the plunger drops controls the pulse force, and the time needed to raise the plunger controls the pulse period. Therefore, there is an interdependence between pulse pressure and period; the difficulty is finding the optimum range.

Emulsification was an unexpected result of pulsing that has only been noticed in the last year. It has been found that an oil-water mixture is formed when pulsing light oils under certain conditions. A goal of this project has been to observe when this happens.

Of a more fundamental nature are the studies on pulsed versus non-pulsed waterfloods. Prior experimental work has demonstrated a substantial flow increase with pulsing, but only for single-fluid systems that do not account for the complex interaction between immiscible phases. Nor is there previous documented work analyzing the final sweep efficiencies of depleted reservoirs. Both of these are addressed in the following thesis.

This work does not attempt to examine pulsing as an environmental remediation tool; rather, the focus has been placed on pulsing as an enhanced oil recovery technique.

1.2 Organization of the thesis

Included in this report is a background to fundamental pulsing theory, prior experimental work, and current laboratory techniques and equipment. Following this, the experimental results are presented and discussed. Finally, conclusions and recommendations for future research are given.

The appendices contain a detailed description of the two Consistent Pulsing Source (CPS) designs, instructions for the CPS, the experimental procedure for the determination of sweep efficiencies, instructions for all experimental cells at the University of Alberta, a Light Non-Aqueous Phase Liquid (LNAPL) environmental experiment, and a suite of chemical assisted, pulsed waterflood tests.

Chapter 2

Background

2.1 Introduction to Pressure Pulsing

In practical terms, pressure pulsing is simply high-amplitude dynamic excitation of a porous medium, which under a pressure gradient increases the flow rate of liquid along the direction of the flow gradient. Mechanical means of excitation involve injecting a low-frequency pulse of fluid into the medium, which is the pressure pulse. This pulse creates many different waves, such as seismic waves. However, it also creates a slow strain wave called the porosity dilation wave, which is the result of interactions and deformations between the fluid and matrix in the porous media. It travels at velocities on the order of 5–150 m/s and is characterized by a spreading front of elastic porosity changes [1].

Figure 2.1 shows the change in pore volume as a porosity dilation wave passes through. This is important because the induced variations in porosity are responsible for the flow rate enhancement effect. As waves of increased and decreased porosity pass through a medium, they induce the pore fluid to flow, significantly increasing flow. In addition to increasing flow, pressure pulsing also has an associated reservoir pressurization effect that is seen in both the field and laboratory [1, 2].

The flow enhancement effect is integrally linked with the reservoir pressurization effect. As the porosity diffusion wave moves through the porous medium, it is accompanied by an increase in pressure. The reason is that as the porosity wave dies off, it leaves the fluid with no place to go. The fluid, in turn, has caused the matrix to elastically compress, which leaves that portion of the reservoir pressurized. It is important to note here that the distance the porosity diffusion wave travels is dependent on variables such as fluid viscosity, confining stress, porosity, permeability, and pore geometry. Therefore, because the confining pressure has been increased in this portion of the reservoir, the next diffusion wave and accompanying fluid can permeate even further. The end result is that the entire reservoir becomes pressurized.

Figure 2.2 is an experiment showing reservoir pressurization in a cylindrical cell packed

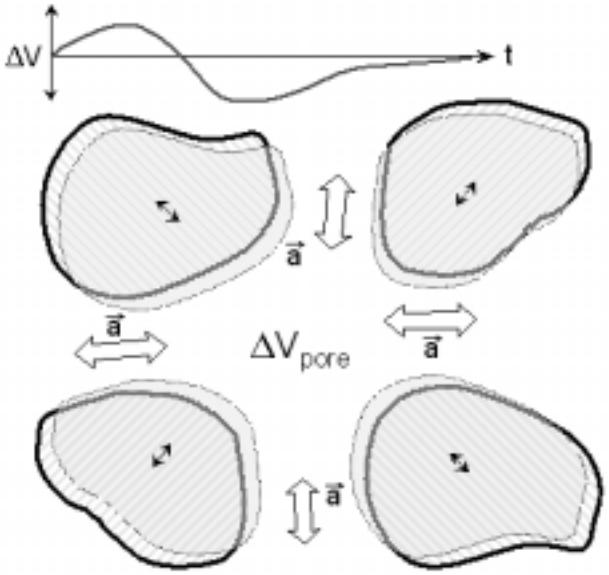

Figure 2.1: Pulsing at the pore scale. As the porosity dilation wave passes through, the pore volume (ΔV) increases and decreases. Figure courtesy of M.Dusseault.

with sieved Ottawa sand. The outflow and inflow were set at a given height and water was run through the system. Three pressure transducers (PT1, PT2, PT3) were mounted on the cell side to monitor reservoir pressure. In the diagram, one can see that the transducer nearest the inflow (PT1) experiences the pressure increase first, after which the pressure permeates through the reservoir. The system is still trying to reach equilibrium when pulsing is discontinued, therefore the peak pressure has still not reached PT2 and PT3. The pressure then dissipates quasi-statically.

For a more detailed explanation of pulsing, it is valuable to look at the de la Cruz - Spanos model. This is the wave propagation theory that predicted the existence of a non-seismic, porosity-pressure dilation wave.

2.2 de la Cruz - Spanos Porous Media Model

The de la Cruz - Spanos porous media model was formulated from basic physical properties to describe wave propagation in porous media [3, 4]. It consists of a complete set of macroscopic equations contructed using volume averaging (see Section 2.2.1). Most importantly, this model includes porosity as a dynamic variable that plays a fundamental role in both the thermomechanics and thermodynamics of the porous medium [1]. The following section explains the basic porous media physics behind pressure pulsing; however, a much more rigorous background can be found elsewhere [3, 4, 5, 6].

The de la Cruz - Spanos model consists of coupled, first order macroscopic equations which

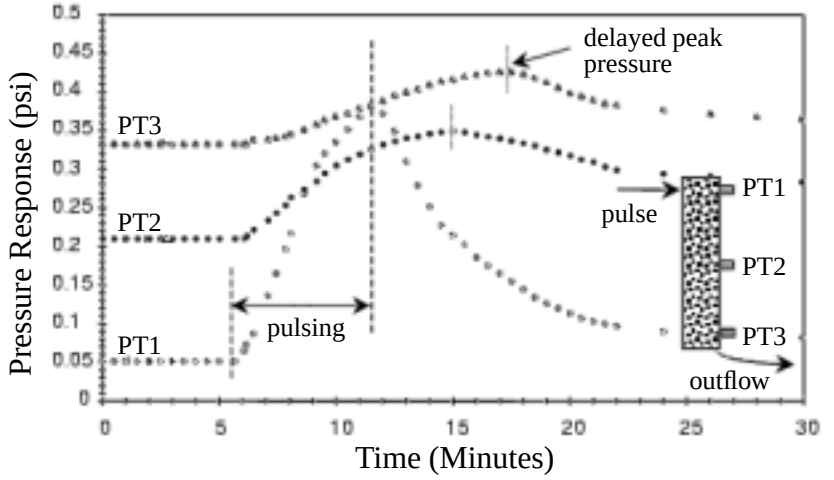

Figure 2.2: Internal pressure response to pulsing at the upstream entry port (data not zeroed). Adapted from Davidson et al., 1999 [1].

describe wave propagation in porous media saturated with a single, viscous, compressible fluid. The equations are:

$$\begin{aligned}\rho_s \frac{\partial^2}{\partial t^2}\vec{u} =& K_s \nabla(\nabla \cdot \vec{u}_s) - \frac{K_s}{1-\eta_0} + \frac{\mu_f \eta_0^2}{(1-\eta_0)K} \cdot \frac{\partial}{\partial t}(\vec{u}_f - \vec{u}_s) \\ & - \frac{\rho_{12}}{(1-\eta_0)} \cdot \frac{\partial}{\partial t^2} \cdot (\vec{u}_f - \vec{u}_s) + \mu_s \left[\nabla^2 \vec{u}_s + \frac{1}{3}\nabla(\nabla \cdot \vec{u}_s)\right] \\ & - K_s \alpha_s \nabla \vec{T}_s\end{aligned} \tag{2.1}$$

$$\begin{aligned}\rho_f \frac{\partial^2}{\partial t^2}\vec{u} =& K_f \nabla(\nabla \cdot \vec{u}_f) - \frac{K_f}{1-\eta_0} + \frac{\mu_f \eta_0^2}{(1-\eta_0)K} \cdot \frac{\partial}{\partial t}(\vec{u}_f - \vec{u}_s) \\ & - \frac{\rho_{12}}{(1-\eta_0)} \cdot \frac{\partial}{\partial t^2} \cdot (\vec{u}_f - \vec{u}_s) + \mu_s \left[\nabla^2 \vec{u}_s + \frac{1}{3}\nabla(\nabla \cdot \vec{u}_s)\right] \\ & - K_s \alpha_s \nabla \vec{T}_s\end{aligned} \tag{2.2}$$

$$\begin{aligned}\rho_s c_v^s \frac{\partial \vec{T}_s}{\partial t} =& T_0 K_s \alpha_s \left[\frac{1}{1-\eta_0}\frac{\partial \eta}{\partial t} - \frac{\partial \nabla \cdot \vec{u}_s}{\partial t}\right] \\ & + \kappa_s \nabla^2 \vec{T}_s + \frac{\gamma}{1-\eta_0}(\vec{T}_f - \vec{T}_s)\end{aligned} \tag{2.3}$$

$$(\rho_f c_p^f - T_0 \alpha_f^2 K_f) \times \frac{\partial \vec{T}_f}{\partial t} = -T_0 \alpha_f K_f \frac{\partial}{\partial t}\left[\nabla \cdot \vec{u}_f + \frac{1}{\eta_0} \cdot \frac{\partial \eta}{\partial t}\right] + \kappa_f \nabla^2 \vec{T}_f - \frac{\gamma}{\eta_0}(\vec{T}_f - \vec{T}_s) \tag{2.4}$$

$$\frac{\partial \eta}{\partial t} = \delta_s \nabla \cdot \vec{\nu}_s - \delta_t \nabla \cdot \nu_f \tag{2.5}$$

Where:

- c_p' is the specific heat, at constant pressure, of the fluid (i)
- c_v^s is the specific heat at constant volume, of the solid (i)
- f is frequency
- k is wavenumber
- K is permeability (ii)
- K_f is the bulk modulus of the fluid (i)
- K_s is the bulk modulus of the solid (i)
- K_d is the bulk modulus of drained material
- K_u is the bulk modulus of undrained material
- $\vec{u}_s$ is the macroscopic solid displacement vector
- $\vec{u}_f$ is the macroscopic fluid displacement vector
- $\vec{\nu}_s$ is the macroscopic solid velocity vector
- $\vec{\nu}_f$ is the macroscopic fluid velocity vector
- V is the averaging volume
- T_s is the macroscopic temperature in the solid
- T_f is the macroscopic temperature in the fluid
- T_0 is the ambient temperature of the porous medium (i)
- α_f if the thermal expansion coefficient for the fluid (i)

- α_s if the thermal expansion coefficient for the solid (i)
- δ_s is the solid dilation factor (ii)
- δ_f is the fluid dilation factor (ii)
- η_0 is the static porosity
- η is the dynamic porosity
- γ is the surface coefficient of heat transfer (ii)
- κ is the effective thermal conductivity across solid-fluid interfaces
- κ_f is the thermal conductivity of the fluid (i)
- κ_s is the thermal conductivity of the solid (i)
- μ_f is the viscosity of the fluid (i)
- μ_s is the shear modulus of the solid (i)
- ρ_s is the density of the solid (i)
- ρ_f is the density of the fluid (i)
- ρ_{12} is the induced mass coefficient (ii)
- ξ_f is the bulk viscosity of the fluid

Equations 2.1 and 2.2 represent the forces acting on macroscopic elements of the interacting continua, while equations 2.3 and 2.4 represent the heat flow in the coupled continua. Equation 2.5 represents the dynamic interaction between relative proportions of solid and fluid constituents and the porosity during a transient compression in the volume element [7].

Both microscopic and macroscopic parameters have been used in these equations. The microscopic parameters, indicated by (i) above, are solely dependent on the solid or fluid phase and are easily determined for simple systems. Macroscopic parameters result from the volume averaging process and are denoted by (ii) above. The variables in equations 2.1 to 2.5 are η, u_s, u_f, $\vec{T}_s$ and $\vec{T}_f$, since $\vec{v}_s$ and $\vec{v}_f$ are simply the time derivatives of $\vec{u}_s$ and $\vec{u}_f$.

The importance and characteristics of the microscopic parameters of porous media are well described in continuum mechanics and thermodynamics literature and will not be described here. A brief description of the main macroscopic properties is given below.

Dynamic Porosity The static porosity (η_0) of a porous medium is constant and generally easy to determine with a sample. The dynamic porosity (η), however, is a variable and represents the first-order change in static porosity when the porous medium is subjected to a transient compression.

Permeability Darcy permeability quantifies the ability of the porous medium to transmit fluids and is easily determined for single-phase fluid flow. In the case of a well-connected porous medium with no macroscopic structures, the permeability parameter (K) represents relative first-order velocities between the fluid and the solid continua, and is equivalent to the Darcy permeability.

Induced Mass Coefficient This coefficient has its origins in the relative accelerations that occur during wave propagation. It appears in Equations 2.1 and 2.2 and accounts for inertial coupling between the phases as a wave passes through them. This parameter is frequency independent, subject to the frequency-wavelength constraints imposed by the de la Cruz-Spanos theory.

The Solid and Fluid Dilation Factors Equation 2.5 states that a change in porosity within a volume element is equal to the difference in the product of the solid dilation factor with the macroscopic change in volume of the solid, and the fluid compliance factor with the macroscopic change in volume of the solid. A macroscopic change in the volume of a phase can be caused by dilation of the constituent or the net flux of the constituent into or out of the volume element. Physical measurements of these factors can be obtained from the undrained and drained bulk moduli (for quasi-static processes).

The Porosity Diffusion Wave The de la Cruz-Spanos porous media model was simplified by neglecting all inertial terms and considering the fluid to be essentially incompressible [6]. The incompressibility of the fluid constraint is satisfied if flow velocity is much less than sound velocity in the fluid. These equations were further manipulated to yield [6]:

$$\begin{aligned} \eta(r,t) &= \eta_0 - \left(1 - \frac{K_d}{K_s}\right) \frac{M_{ik}}{K_d + 4\mu_s/3} \\ &\quad \times \left\{ \frac{r_i r_k}{r^5} \frac{2}{\pi^{3/2}} \int_{r/2\sqrt{Dt}}^{\infty} dy y^4 e^{-y^2} - \frac{\delta_i k}{r^3} \frac{1}{\pi^{3/2}} \int_{r/2\sqrt{Dt}}^{\infty} dy y^2 e^{-y^2} \right\} \end{aligned} \tag{2.6}$$

Where M_{ik} is the seismic moment tensor and D is the porosity diffusion coefficient, which is equal to:

$$D = \frac{k}{\mu_f} \frac{K_s(1-\eta_0)\left[K_d + (4\mu_s/3)\right]}{\eta_0[\eta_0 K_s + (1-\eta_0)(K_s - K_d)}$$

and

$$y^2 = \frac{r^2}{4} D(t-t')$$

This equation represents the dynamic porosity as a function of the seismic moment applied to a fluid saturated porous media.

The above expressions were further analyzed to derive an expression for the pressure regime within a fluid saturated porous medium subjected to a quasi-static stress[5]. This expression is valid for a pure shear fracture with slip in the x-direction and normal to the plane of slip in the z-direction, and at a point with coordinates $r = (x, 0, z)$.

$$\rho_f(x, z; t) \approx \frac{\mu_s b S}{10\pi\eta_0 (Dt)^{3/2}} \frac{n_x n_z}{\sqrt{\pi/p^2} + 2/3\rho^3} \tag{2.7}$$

Where:

$$\rho^2 = \frac{x^2 + z^2}{4Dt}$$

and n_x and n_y are direction cosines from the source to the observing point.

Equation 2.7 shows that a pulse of pressure propagates from a fracture source and the maximum value of this pressure travels as $r_m \infty \sqrt{Dt}$ and decreases in amplitude as $(Dt)^{1/2}$. The traveling pulse increases pore pressure for a brief time within the fluid filled pores of the porous media and causes pore dilation. This results in a diffusional front that causes a variation in porosity to spread from the point of failure. Over time, this failure leads to a static change in porosity, which decays with distance from the source to the point of observation as r^{-3} [6].

More recently the dynamic limit of incompressible fluid motions has been studied. In this case, one obtains a tsunami-like wave which is predicted to move at speeds of approximately 100 m/s in heavy oil reservoirs. This wave is symbiotically coupled to the quasi-static porosity diffusion process, which traps the mechanical energy of successive pulses, resulting in an increased reservoir pressure.

2.2.1 Volume Averaging

The de la Cruz - Spanos theory depends on volume averaging, which is introduced here. Volume averaging is used to reformulate problems at a larger scale by filtering out the overabundance of physical detail at the pore-scale in such a manner that no specific reference to pore-scale motion remains [8]. The method was pioneered by the work of Hubbard [9], Whitaker [10, 11], and Slattery [12].

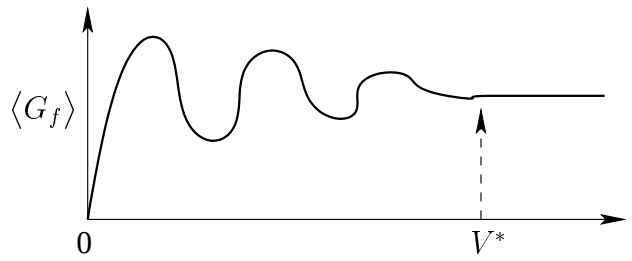

Figure 2.3: Minimum volume required (V^*) for the volume element $\langle G_f \rangle$.

In the volume averaging procedure, one constructs volume regions V in the porous medium of identical shapes, volumes, and orientations. These are then ascribed an average value for physical quantities within the volume V to a point x, which uniquely defines V. For example, de la Cruz and Spanos assume V to be spheres and each V is specified uniquely by the center of the sphere x. Also by choosing spheres, the problem of orientation is avoided. If we assume $G_f(x)$ to be a physical quantity of the fluid and that $G_f(x)$ equals zero everywhere outside the fluid, the volume average of G_f over any region V is defined as:

$$\langle G_f \rangle = \frac{1}{V} \int_V G_f(x) dV \tag{2.8}$$

where $\langle G_f \rangle$ is a function of the center of the volume elements [8].

If one assumes that the center of the volume element is within the solid and plot $\langle G_f \rangle$ as a function of the radius of the volume V one might obtain a curve similar to Figure 2.3.

Since the center of the volume V was assumed to be in the solid, then $\langle G_f \rangle$ is assumed to be zero at the origin. As one starts increasing the volume size, portions of the fluid are contained within the volume, and $\langle G_f \rangle$ increases from zero through fluctuations due to random distribution of fluid at the pore-scale. For values of V larger than V^*, the pore-scale variations are smoothed out, and therefore a restriction that $V > V^*$ is imposed. The volume V^* is referred to as the minimum representative elemental volume.

2.3 Secondary and Tertiary Oil Recovery

Natural oil production mechanisms vary widely due to the inherent variability of each oil reservoir. The differences in host rock and oil type necessitate different approaches to oil production, some of which are briefly reviewed here. First, an overview to conventional and heavy-oil reservoir production is given.

2.3.1 Conventional Light-oil Reservoirs

In conventional light-oil reservoirs, the first recovery step is called primary production, which refers to oil removal through the use of natural driving mechanisms in the reservoir. Secondary recovery techniques use water floods or gas injection, to remove additional oil. Water floods involve pumping water into injection wells to displace oil to the production well and gas injection is done by injecting gas into the gas cap to increase the natural driving forces. After completion of primary and secondary recovery processes in conventional light-oil reservoirs, typically 30–80% of the Original Oil In Place (OOIP) remains in the porous rock and sand of the reservoir [13]. A portion of this oil can then be removed with tertiary or enhanced oil recovery methods. This includes such processes as gas injection (miscible or inert), chemical processes [14, 15], and thermal recovery (steam) [16, 17, 18]. Some more exotic tertiary recovery processes include microbial, electrical heating, mining, and combustion. The term Enhanced Oil Recovery (EOR) is generally used when these methods immediately follow primary production.

2.3.2 Heavy-oil Reservoirs

The stages of production in heavy-oil reservoirs are slightly different. A few years ago, it was generally accepted that primary production was not viable in heavy oil reservoirs because of the inability of high viscosity oils to flow through the reservoir. However, in cases were solid and fluid are being removed from the production well (solid flow), there have been very successful primary production wells in heavy oil reservoirs [19, 20]. In heavy-oil primary production, the reservoir is then observed to undergo crumbling of the matrix and the formation of wormholes (high permeability fingers extending from the production well) which result in a substantial increase in fluid production. However, in cases where primary production is an effective heavy oil recovery technology, it might also be followed by thermal recovery processes. The principal thermal recovery techniques are steam drive, cyclic steam injection, which is typically followed by steam drive once communication between wells has been established, and steam assisted gravity drainage [13].

2.3.3 Tertiary Recovery

Tertiary recovery methods are employed at the stage when substantial amounts of residual oil remains trapped in disconnected regions of the reservoir, which may vary from the pore scale to major portions of the reservoir. Some of the more conventional methods used to recover a fraction of this trapped oil are discussed here.

Miscible Gas Floods

Miscible gas floods have been performed using three different schemes. The first approach involves the continuous injection of a miscible gas until the oil production ceases to be economical [21]. In the second approach, a slug of miscible gas is followed by a less expensive chase gas [22]. However, the viability of this scheme is strongly dependent on the stability of the macroscopic front between the gases. The third scheme involves alternating the injection of water and gas (WAG).

Inert Gas Injection

Inert gas injection has been proposed as a driving mechanism for more expensive miscible gas slugs. Another use has been demonstrated in the laboratory experiments where the gas has been shown to pass through the water phase along fine pore-scale flow channels. Here trapped oil spreads along the surface of these channels and if they are aligned vertically then an oil bank forms due to gravity drainage [13].

Surfactant Processes

In surfactant processes, a low concentration surfactant solution (1% or less) is injected into the reservoir [23]. The objective of this process is to decrease oil-water interfacial tension and thereby reduce capillary barrier effects. A micro-emulsion or micellar flood refers to processes where a concentrated surfactant solution (10% or more) and a co-surfactant (usually high molecular weight alcohol) are injected into the reservoir. In these cases, the goal is to emulsify oil as well as to reduce capillary effects.

Caustic Floods

Caustic flooding is the injection of an alkali (caustic solution) into the reservoir, resulting in the *in situ* formation of surfactants that decrease the oil-water interfacial tension (see Surfactant Processes). The reservoir oil must contain organic acids for this to work [13].

Steam Drive

Steamflooding is widely used in the recovery of heavy, viscous oils and has been a very successful recovery technique [7], although it is not used on any substantial scale in Alberta and Saskatchewan. It consists of the continuous injection of steam directly into the reservoir. The steam heats up areas close to the injection wellbores, which provides an oil-drive mechanism, reduces the viscosity of oil in place, and often increases the absolute and relative permeability of the surrounding reservoir matrix by thermal stress dilation. The end result is increased flow

of oil to the pumping wellbores. Generally, when wells are optimally spaced and the reservoir properties are suitable, this process is cost effective [7].

Steam Assisted Gravity Drainage (SAGD)

SAGD is a process where heated oil flows from around growing steam chambers, driven by gravity segregation, to lower horizontal wells. It can also be characterized as a counter-current process where oil moves in a direction opposite to that of the steam front advance [7]. A simple SAGD process typically utilizes two horizontal wells, an injector and a producer, drilled into the lower part of the formation. Steam injected into the upper well increases the mobility of contained oil in a continuously enlarging "steam chamber". Gravity provides the drive mechanism for the mobilized oil and condensed water, which drain continuously into the lower well, with the voidage being filled with exolved gases and live steam [7].

Cold Heavy-Oil Production with Sand (CHOPS)

Cold heavy-oil production with sand involves producing a part of the unconsolidated reservoir matrix together with heavy crude oil. This is hypothesized to result in a zone that is dilated and of enhanced permeability, or in the formation of "wormholes" or channels. These processes increase the permeability of the reservoir, which facilitates the flow of the viscous and foamy oil into the wellbore. The foamy oil is the result of gas exsolution as bubbles [24].

2.4 Previous Laboratory Work

Most experimental work prior to this study can be found in Davidson *et al.*, 1999 [1]. Some additional documentation can be found in Woynillowicz, 2000 [25]. In general, the early experimental goals covered the following areas:

- Verification of the underlying physical theory,
- Observations of the effects of pulsing,
- Quantitative analysis of pulsed, one-fluid flow, and,
- Experimental cell construction and pulse source optimization.

The following sections include some highlights of these early results, as well as some background experimental work done at the beginning of this study. However, the quantitative analysis of pulsed one-fluid flow is not covered (see Davidson et al., 1999 [1]), nor is the experimental

cell construction. Instead, the topics of pulsing sources, flow enhancement, reservoir pressurization, and viscous fingering are reviewed. Section 2.4.4 contains all of the previous experimental conclusions.

2.4.1 Pulsing sources

Early experiments relied on "hammer pulsing", which involved compressing Tygon^{TM} tubing with a mallet before the inflow. The squeeze or impact did not fully close the tube and stop flow (Figure 2.4), nor was it supposed to create a "milking" action (peristaltic effect). The high amplitude impulse was dominated by low frequencies which propagated in both directions from the impact point. As the impulse entered the porous medium, it was converted to a porosity diffusion wave accompanied by a small pressure change. The downside of hammer pulsing was that it required manual operation, resulting in inconsistent frequency and force. It was also not practical for longer experiments involving heavy oils, which could last for several hours. As a result, the first goal for the current study was to build a consistent pulsing source.

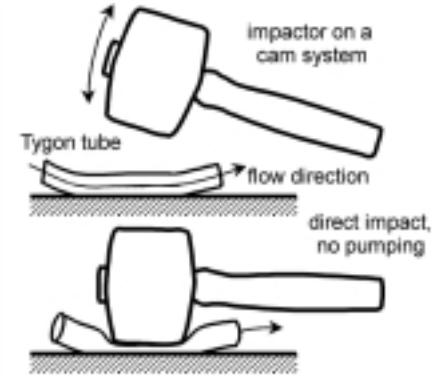

Figure 2.4: The basics behind hammer pulsing, which was the pressure pulse generation method before the consistent pulsing source [1].

2.4.2 Flow Enhancement

Figure 2.5 is a series of two experiments done to show the flow enhancement effect of pulsing. In these photos, one can see both pulsed and non-pulsed waterfloods in a water-wet system. The test variables include a porosity of 35.5%, mineral oil with viscosity 32 cP, and 20–30 mesh sieved Ottawa sand. A clock has been placed in the lower-left hand side to enable comparison. As one can see in the figure, the pulsed system is completely through the experimental cell after 210 seconds, but the non-pulsed test is still just starting. It is worth noting that if pulsing had been discontinued, the flow rate would have slowly decayed back to static flow levels [1]. This

is because there are no permanent changes to the matrix, and the flow rate decay is a function of the reservoir pressurization effect.

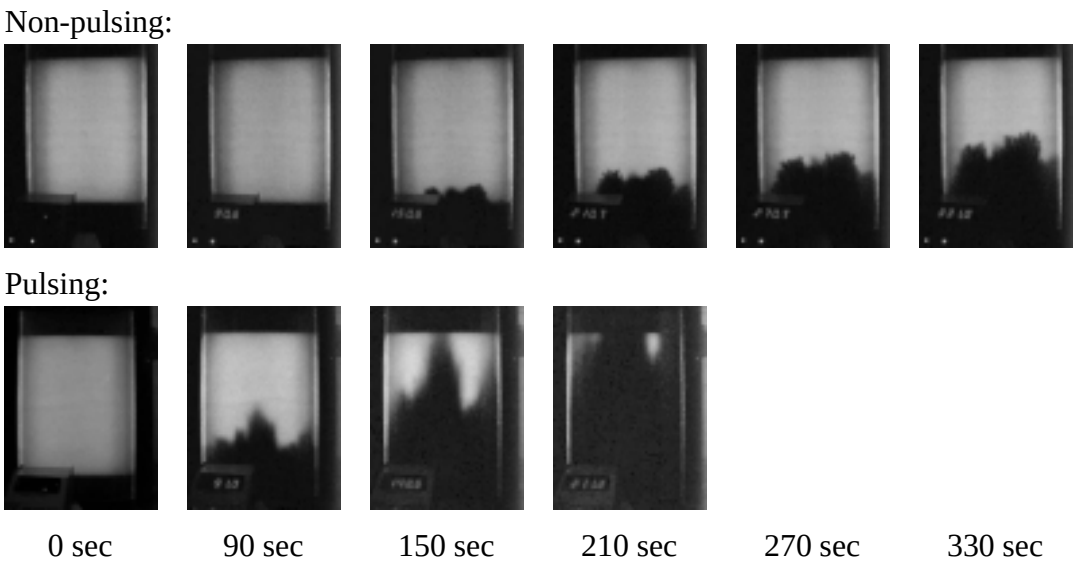

Figure 2.5: Non-pulsed and pulsed waterfloods into a water-wet system. Photos of the pulsed experiment were not taken after 210 seconds because the displacement front was completely through.

2.4.3 Viscous Fingering

Taylor [13] showed theoretically that when two superposed fluids of different densities are accelerated in a direction perpendicular to their interface, that the interface will be stable or unstable depending on whether the acceleration is directed from the more dense to the less dense fluid or vice versa. If the dense fluid is pushing the less dense fluid, the resulting instability is referred to as a Taylor instability, or viscous fingering. Figure 2.6 shows an experiment very similar to the flow enhancement test in Figure 2.5. The only difference is that the viscous fingering experiment has been done in an oil-wet environment, not a water-wet environment. Viscous fingering is more important to the oil-wet system because the water has to displace the oil rather than disperse through it using the existing water concentration.

In Figure 2.6, ones sees that the viscous fingers have been suppressed in the pulsed experiment, indicating that a much larger portion of the oil reservoir has been contacted by the displacing phase (*i.e.* higher sweep efficiency). Furthermore, one can see the strong flow enhancement due to pulsing.

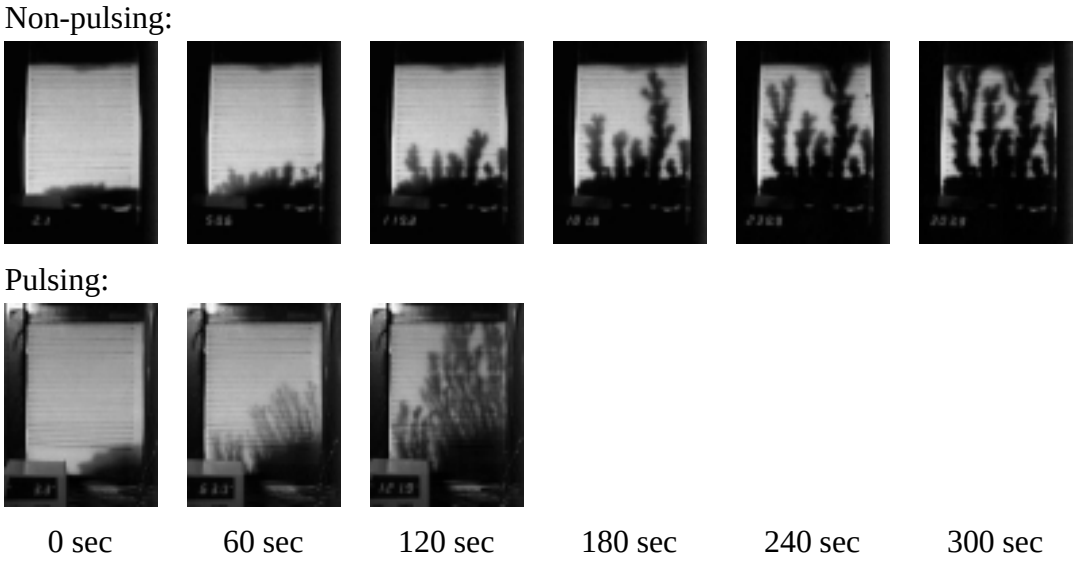

Figure 2.6: Non-pulsed and pulsed waterfloods into an oil-wet system. Photos of the pulsed experiment were not taken after 120 seconds because the displacement front was completely through.

2.4.4 Previous Experimental Conclusions

The previous experimental conclusions, which have been taken directly from Davidson et al., 1999, are:

- Large flow rate enhancements occur when using large-strain, non-seismic excitation in porous media;
- These flow rate enhancements are because of the dynamic excitation of the fluid phase, increasing the internal pressure and the flow rate;
- Strain levels must be greater than 10^{-5} for the effect to be substantial, far above typical seismic strains (10^{-7}–10^{-10});
- The energy source can be a pressure pulse or a strain pulse: because of solid-fluid coupling at the pore scale, conversion occurs, and they are *de facto* equivalent;
- Impulses dominated by a range of low frequencies are needed for heterogeneous porous media (conversely, single frequency sinusoidal excitation is less effective);
- Viscous fingering instabilities can be substantially modified by pressure pulsing (this was proven by introducing less viscous fluids into a system by pulsing, and noting that instead of channeling, dispersion was favored);

- A detectable porosity diffusion wave is generated by each impulse, and this wave has a velocity in line with predictions of the theory: in the laboratory under low stress (0.5 MPa), velocities of 8–10 m/s were observed;
- A detectable porosity wave (a “tsunami”) diffuses through the system. If the wave magnitude is large enough it generates a synergetic internal pressure build-up in the flowing system, changing the pressure gradient from “steady-state” conditions to one where the exit gradients and internal pressures are larger;
- The process is repeatable (reversible) with no changes in phase saturations or in sand pack fabric;
- The process seems relatively more effective in viscous oils, as compared to low-viscosity oils;
- Flow rate enhancement occurs in all liquids, and at all particle sizes tested; and,
- The permeability of the system and the magnitude of the external head dominate the absolute flow rate and post-excitation pressure decay behavior. (In other words, Darcy’s law is perfectly valid in these sand packs for “quasi-static” flow that is not dynamically enhanced.)

Chapter 3

Experimental Equipment and Setup

To attain quantitative and repeatable results, experimental tests must be consistent. To this end, two important achievements have been the development of a consistent experimental methodology, and the construction of a Consistent Pulsing Source (CPS). The experimental equipment, setup, and CPS are all described in the following section. Also included is an overview of the test variables. Lab procedures and a more detailed look at the CPS can be found in Appendices C and A, respectively.

3.1 Experimental Setup

The experimental setup is best explained with the aid of Figure 3.1. The pressure drop (Δp) across the experimental cell is maintained by a large-volume reservoir suspended at a fixed height above the end of the outflow: the height difference is the head, $\Delta p]_{total} = \rho g \Delta h$, and the large volume reservoir means that $\Delta p]_{total}$ remains constant throughout the test. Flow rates at the outflow are measured using graduated cylinders and the fluid pulses are provided by the CPS, which is integrated with the large-volume reservoir. The CPS is explained in Section 3.3 and Appendix A. Not pictured is the large, steel, stiffening bracket that prevents the Lucite^{TM} sides from bowing out during an experiment.

The medium within the experimental cell consists of sand or glass beads, which are sieved to help ensure a consistent porosity. During this study, it has been found that porosity changes as small as 0.5% affect sweep efficiency. Glass beads are often used because their smooth surface and consistent pore size results in a more consistent and homogenous hydraulic conductivity.

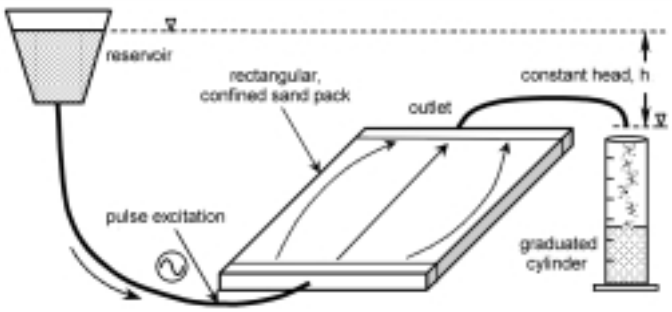

Figure 3.1: The experimental setup showing the large-volume reservoir, the outflow and graduated cylinder, and the experimental cell. Pulsing is provided by the CPS, which is integrated with the water reservoir. Figure adapted from Davidson, 1999 [1].

3.2 Experimental Cell

The experimental cell used for these studies is rectangular in shape and uses parallel plates (250mm$\times$320mm) of Lucite^{TM} 20 mm apart that are placed vertically and filled with sand (Figure 3.2). The sand is packed as dense as possible in water using vibro-densification. Once filled, the end platens that control the in-plane flow conditions are replaced, so that the sand is held rigidly in place. The porosity of the cell is set by adjusting the end platens to get the desired volume. Porosity is calculated by dividing the medium volume by the total volume in the cell. An advantage of this cell is that it can be photographed under backlit conditions to give an idea of frontal displacement efficiency. More photos of the standard experimental cell can be found in the appendices (Figures C.1 and C.2). Other experimental cells, which are occasionally used for heavy oil or demonstration purposes, are shown in Appendix D. More detailed instructions are included in Appendices B, C, D, and F.

Towards the end of the study, a pressure transducer was mounted on the cell inflow to monitor ingoing pulses. It is pictured with the pressure gauge, which was used to ensure consistent pulse amplitudes, in Figure 3.3.

3.3 The Consistent Pulsing Source (CPS)

The construction of a Consistent Pulsing Source (CPS) was one of the first major tasks to be addressed. The CPS went through two major designs, the first being piston-actuated, and the second using compressed air. The piston design failed as a useful tool in the lab. It was heavy, not automated, incapable of controlling pulse duration, difficult to use, and time-consuming to create. The second design took a completely different approach.

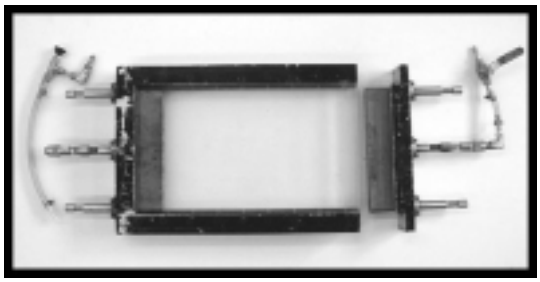

Figure 3.2: The standard cell, which is used for almost all experiments due to its ease of use. The main body of the cell is composed of clear Lucite^{TM}, the steel on the edges only acts as support. During experiments, an additional, thick, stiffening bracket is placed on the Lucite^{TM} walls to prevent the sides from bowing out. On one side, the end platen has been removed allowing the inner reservoir to be seen. The reservoir can be moved to compress the matrix during experiments.

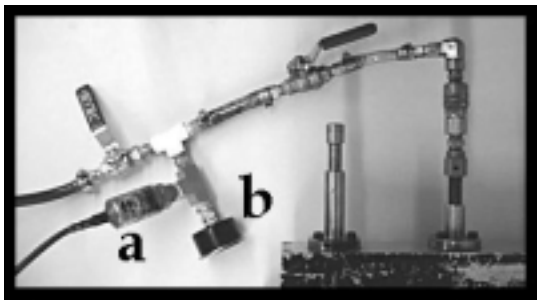

Figure 3.3: The inflow on the standard experimental cell. Labelled are the a) 10 psi pressure transducer and the b) pressure gauge used for monitoring pulse pressures.

The compressed-gas CPS is integrated with the water reservoir already shown in Figure 3.1. Quickly pressurizing and depressurizing the reservoir using compressed air creates dampened pressure pulses (Figure 3.3). In this way, one can easily control the force generated, the pulse duration, and the pulse frequency. Not only is it automated and easy to control, but the use of only one reservoir makes the second CPS easier to use. A more detailed description of both the first and second designs can be found in Appendix A.

Unfortunately, the current CPS also has its limitations. As a test progresses, the reservoir water level decreases, leaving more air at the top of the reservoir. The highly compressible air results in longer reservoir pressurization times, leading to shorter and weaker pulses (Figure 3.3). Direct solutions, which aimed at maintaining a consistent water level, either failed or were difficult to implement. Instead, an indirect solution is used to compensate. The air pressure supplied to the water reservoir is steadily increased, giving a consistent pulse pressure, frequency,

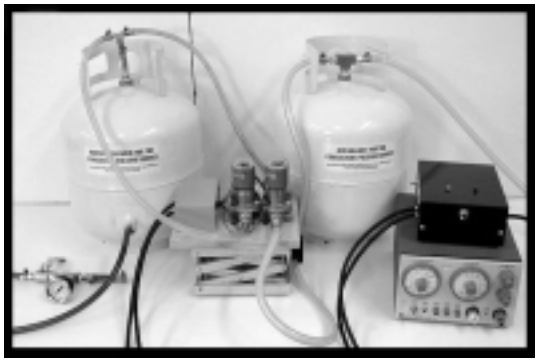

Figure 3.4: The compressed-gas CPS. The two tanks are the water reservoir and air accumulator and the two solenoid valves are for controlling air pressure in the water reservoir. Finally, there is a square-wave generator with a relay box on top of it that controls the solenoid valves. The square-wave generator was eventually replaced by a computer.

and period. However, once three liters of water have been used, the increase in air pressure can no longer compensate for the longer pressurization times. At this point, the experiment is briefly paused and the water reservoir refilled. This affects the final results, because pausing the experiment causes the experimental cell to lose pressure built up by pulsing. This results in lower flow rates, because the pressure increase is linked to the flow increase. This problem is discussed further in Section 5.1. Clearly, a better solution should be found for longer experiments.

3.4 Sweep Efficiency

Sweep efficiency is an important parameter for pulsing experiments because it provides a measure by which to gauge results. It is defined as the total volume fraction of a reservoir model contacted by the displacing phase [26]. For a waterflood displacing an oil-saturated medium, one can express the sweep efficiency as:

$$Efficiency = 100\% \times \left[\frac{V_{out}}{V_{initial}}\right] \tag{3.1}$$

where V_{out} is the total volumetric outflow of oil out of the cell and $V_{initial}$ is the total volume of oil initially in the cell.

3.5 Test Variables

There are more test variables than can be accounted for in this experimental program, especially when considering that lab preparation, execution, and clean-up can easily take two days. The

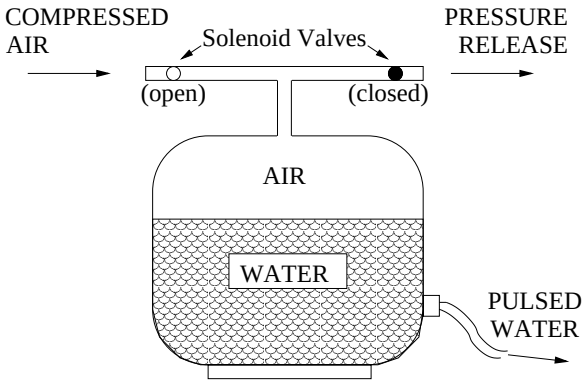

Figure 3.5: Basics of the CPS operation. Pulses are made by quickly opening the compressed air solenoid valve while simultaneously closing the pressure release solenoid valve. This sends a quick pulse of fluid through the outflow at the bottom. Static head between pulses is achieved by reversing the operation; in other words, closing the compressed air valve and opening the release valve.

test variables include:

- Fluid viscosity
- Static head
- Porosity
- Pulse pressure
- Pulse period (frequency)

Paraffin oil has been used for all experiments and the static head has been arbitrarily kept at 1 meter for almost all experiments. The properties of paraffin oil compared with water are shown in Table 3.1. Some experimental work has been done with the last three variables, so these change from test to test. In the case of porosity, some experiments use 20–30 mesh sand or glass beads, and some experiments use finer, 30–40 glass beads. The pulse pressure is varied from 3.5–7.5 psi, and the pulse period is varied from 0.75–1.2 seconds.

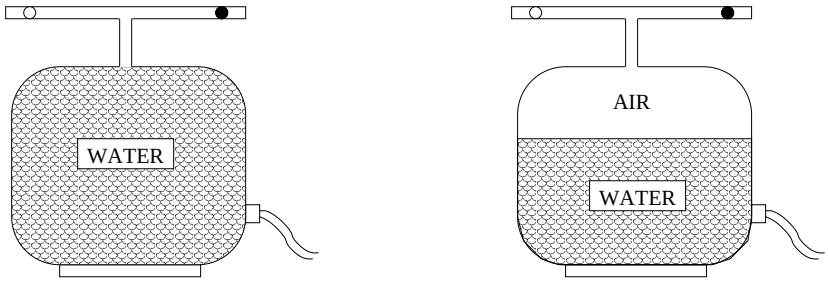

(a) Initial water level: no air compressibility, therefore sharp fluid pulses

(b) Final water level: air compresses, therefore fluid pulses lose sharpness (exaggerated scale)

Figure 3.6: The CPS water reservoir problem. There is currently no way of maintaining the water level during pulsing. If the air pressure being supplied to the CPS remained constant, the increasing air volume at the top of the reservoir would result in decreasing pulse pressures. To compensate for this, the pulse pressures are monitored and the air pressure being supplied is increased accordingly. The result of this is discussed and shown in Section 5.1.3.

Table 3.1: Paraffin oil and water properties (pressure 1.013×10^{-5} N/m^2 and temperature 288.15 K).

Property	Water	Paraffin Oil
Mass Density [kg/m^3]	1000	800
Specific Weight/Gravity [N/m^3]	9814	7851
Coefficient of Dynamic Viscosity [kg/m·s]	1.14×10^{-3}	1.9
Kinematic Viscosity [m^2/s]	1.14×10^{-6}	2.375×10^{-3}
Surface Tension [N/m]	0.028	0.072

Chapter 4

Laboratory Results

There were two distinct phases in the laboratory program. Phase I focused on the development of the experimental equipment and lab methodologies, which allowed accurate and consistent results to be collected. These results then formed the basis for Phase II: quantitative analysis.

4.1 Phase I: Equipment and Experimental Procedure Development

Phase I involved approximately 50 tests and lasted from mid-March until mid-August 2000, which is close to five months. In that time, the first and second CPS designs were built and tested and the experimental procedure was refined. Some experiments focused on heavy-oil or environmental applications (Appendix E), while others verified physical theory (Chapter 2: Background). However, many of these 50 results are not reported here, either because they were done using hammer pulsing, or they were used to develop the failed piston CPS (Appendix A).

Phase I results were not used in the quantitative analysis because changes in the lab equipment or test methodology made comparison impossible. These changes, and the reasoning for their implementation, are presented in chronological order here:

1. **Compressed-gas CPS**
   This enabled accurate and quantitative comparison between pulsed two-fluid phase systems. Previously, it had been impossible to ensure consistent pulses.

2. **Compression bracket**
   The compression bracket prevented the experimental cell walls from bowing out during experiments and ruining porosity calculations. Porosity measurements previous to this may have been as much as 1% off. Pictures of the compression bracket can be found in Appendix F, Figures F.2.2 and F.2.3.

3. **Constant pulse pressure**
   Due to a limitation of the CPS, pulse pressures tended to decrease during an experiment (Section 3.3). An inflow pressure gauge was added to allow pulse pressures to be monitored and corrected.

4. **Oscilloscope**
   After the acquisition of an oscilloscope, it was found that pulse generator readings were incorrect. The error in pulse frequency/pulse period measurements before this was quite significant (as much as 0.25s).

5. **Glass beads**
   Before the glass beads, it was extremely difficult to get consistent results. Not only were the glass beads easier to use and slightly more consistent than sand, but they were also less expensive. This marked the beginning of Phase II.

6. **Reservoir-depletion experiments**
   These experiments allowed for the quantification of the final sweep efficiency, which has proved to be an important variable for comparison.

7. **Pressure transducers and full PC automation**
   The pressure transducers made measurement of the inflow and outflow pulses possible. Additionally, the PC replaced the square-wave generator (see Section 3.3), which had been difficult to calibrate with the oscilloscope.

The end of Phase I was marked by the use of glass beads, which finally gave tests the consistency required to make meaningful comparisons. However, even during Phase II there were many experiments that could not be used, either because they were too short, the wrong porosity, or one of the variables was changed and thereafter abandoned.

Table 4.1 shows all tests that have been done since the construction of the compressed-gas CPS. Take special note of the † symbol, which indicates inaccurate measurements, and the ‡ symbol, which indicates tests that have been used in analysis. Numbers under the Porous Medium column, such as 20-30, refer to the sieve mesh sizes. All tests have been paraffin oil saturated with a residual connate water concentration. Only water has been used as the injection fluid, therefore all results may be considered simulations of pressure pulse waterfloods.

Table 4.1: Summary of experiments since the construction of the compressed-gas CPS. Comments have been added at times when there was a major change in testing equipment or methodology.

Date	Pulse Pressure [psi]	Pulse Duration /Period [sec]	Porous Medium	Porosity [%]	Comments
4.7.00		*non-pulsed*	Unsieved sand	34.0 †	Using unsieved sand because it is cheap and the CPS is still under development
5.7.00	3 †	0.25/1.25 †	Unsieved sand	34.5 †	First test with the compressed-gas CPS
6.7.00			Unsieved sand	34.5 †	Hand (mallet) pulsing test for comparison with the CPS.
18.7.00	8 †	0.25/0.75 †	Unsieved sand	34.9 †	
19.7.00	5 †	0.25/0.75 †	Unsieved sand	34.1 †	For comparison with 18.7.00. 3 psi pressure variation
25.7.00			Unsieved sand		Tried putting solenoids below reservoir. Failed because valves are asynchronous
27.7.00	8 †	0.25/1.0 †	Unsieved sand	32.9 †	For comparison with 18.7.00. Porosity seems largely accountable for the test differences.
31.7.00	8 †	0.25/0.75 †	Unsieved sand	33.1 †	Air ballast tank (accumulator) added to decrease pressurization times.
		A compression bracket was added to prevent the cell walls from bowing out. All porosity measurements prior to this were incorrect.			
8.8.00	5 †	0.25/0.75 †	Unsieved sand	34.6	New pressure gauge added to inflow, previous pressure values inaccurate.
9.8.00	3 †	0.25/0.75 †	Unsieved sand	35	

†*inaccurate measurement;* ‡*experiment used in the main report*

continued on next page

Table 4.1: (continued)

Date	Pulse Pressure [psi]	Pulse Duration /Period [sec]	Porous Medium	Porosity [%]	Comments
10.8.00	5.5 †	0.25/1.0 †	Unsieved sand	34.2	
	Started ensuring pulse pressures stayed constant during testing. Previously, they dropped off as the test progressed.				
11.8.00	7.5	0.25/0.75 †	Unsieved sand	34.9	First test with constant pulse pressures.
14.8.00	6.5	0.25/0.75 †	Unsieved sand	33.7	
	Started using an oscilloscope to correct pulse generator measurements.				
16.8.00	6.5	0.25/0.76	Unsieved sand	37.1	
17.8.00	6.5	0.25/0.76	< 30 sand	33.8	Using sieved sand because relatively small porosity variations are capable of seriously affecting the results
18.8.00	5	0.25/0.76	> 30 sand	34.3	Switched to > 30 mesh because it is faster to sieve
21.8.00	6	0.25/0.76	> 30 sand	34.8	Could not constrain the porosity. It appears that a 0.5% change in porosity has a greater effect than a 1 psi pressure change.
23.8.00	6.5	0.25/0.76	20-30 sand	36.7	Switched to 20-30 sieved sand, but time consuming to sieve and too costly to buy pre-sieved.
	Started using sieved glass beads to minimize the porosity variations.				
24.8.00	6.5	0.25/0.76	20-30 beads	36.3	
29.8.00	6.5	0.25/0.76	20-30 beads	36.3	First time a consistent porosity has been achieved.
30.8.00 ‡	6.5	0.25/0.76	20-30 beads	36.3	Third test in a row using the same conditions. Results show a large degree of variation.
31.8.00 ‡	7.5	0.25/0.76	20-30 beads	36.2	Higher pressure test.

†*inaccurate measurement;* ‡*experiment used in the main report*

continued on next page

Table 4.1: (continued)

Date	Pulse Pressure [psi]	Pulse Duration /Period [sec]	Porous Medium	Porosity [%]	Comments
11.9.00	7.5	0.25/0.76	20-30 beads	37.1	First test in new lab. Forgot to tighten bottom reservoir, porosity too high.
14.9.00 ‡	6.5	0.25/1.0	20-30 beads	36.2	Longer pulse period.
18.9.00	6.5	0.25/1.0	20-30 beads	36.3	Lower hydraulic head (0.5m instead of 1m).
19.9.00	6.5	0.25/0.75	20-30 beads	36.0	Some fine-grained silica accidentally added to sample, porosity off. Lower hydraulic head (0.5m).
21.9.00 ‡	7.5	0.25/0.75	20-30 beads	36.1	Higher pressure test (same as 31.8.00).
22.9.00	6.5	*non-pulsed*	20-30 beads	36.1	No pulsing, just an 8.5psi waterflood.
25.9.00 ‡	6.5	0.25/0.75	20-30 beads	36.2	
26.9.00 ‡	5.5	0.25/0.75	20-30 beads	36.3	Test with lower pulse pressure.
28.9.00 ‡	6.5	0.25/1.25	20-30 beads	36.4	Pulser broke down after 120s. Continued with experiment on October 2.
3.10.00	6.5	0.25/0.65	20-30 beads		Shorter period. Appears to be problem with pressurization at short periods.
4.10.00	6.5	0.25/0.75	20-30 beads		Oil company demo.
16.10.00	6.5	0.25/0.75	20-30 beads	36.1	Oil company demo.
18.10.00	6.5	0.25/0.75	20-30 beads	36.2	Oil company demo.
29.10.00	-	*non-pulsed*	20-30 beads		Not long enough. Experiment on 1.11.00 replaced this one.
	Started doing long-term (reservoir-depletion) experiments. Used to determine the ultimate reservoir sweep efficiency.				
1.11.00 ‡	-	*non-pulsed*	20-30 beads	35.9	

†*inaccurate measurement;* ‡*experiment used in the main report*

continued on next page

Table 4.1: (continued)

Date	Pulse Pressure [psi]	Pulse Duration /Period [sec]	Porous Medium	Porosity [%]	Comments
3.11.00 ‡	6.5	0.25/0.75	20-30 beads	35.8	
8.11.00 ‡	-	*non-pulsed*	30-40 beads	35.5	Found more containers, ran experiments even longer - better results.
10.11.00 ‡	6.5	0.25/0.75	30-40 beads	35.2	
6.02.01	6.5	0.25/0.75	30-40 beads		Oil company demo
Started automating tests with the PC and Labview^{TM}. An inflow and outflow transducer were also added					
6.03.01	4.5	0.25/0.75	20-30 beads		Discovered the solenoid valves were mis-wired 2 minutes into the test. The test had to be discarded.
12.03.01 ‡	3.5	0.25/0.75	20-30 beads	36.2	Test at a lower pulse pressure. Porosity was higher to match earlier tests.
4.04.01 ‡	6.5	0.25/1.0	20-30 beads	35.8	Longer pulse period.
8.04.01 ‡	6.5	0.25/0.75	20-30 beads	35.8	Longer duration than 3.11.00
The following are the chemical assisted, pulsed waterflood tests (Appendix F). They were done with heavy oil instead of paraffin oil.					
13.07.01	5.5	0.25/0.75	30-40 beads	35.5	Failed chemical test, used the wrong concentration.
15.07.01	5.5	0.25/0.75	30-40 beads	35.5	Pulsed water test.
17.07.01	5.5	0.25/0.75	30-40 beads	35.5	Chemical A pulsed test.
18.07.01	5.5	0.25/0.75	30-40 beads	35.5	Chemical B pulsed test.
19.07.01	5.5	0.25/0.75	30-40 beads	35.5	Chemical C pulsed test.
20.07.01	*non-pulsed*		30-40 beads	35.5	Waterflood, no pulsing.

†*inaccurate measurement;* ‡*experiment used in the main report*

continued on next page

Table 4.1: (continued)

Date	Pulse Pressure [psi]	Pulse Duration /Period [sec]	Porous Medium	Porosity [%]	Comments
25.07.01	5.5	0.25/0.75	30-40 beads	35.5	Chemical B test, different concentration.
8.08.01	*non-pulsed*		30-40 beads	35.5	Chemical A non-pulsed test.
10.08.01	5.5	0.25/0.75	30-40 beads	35.5	Chemical A pulsed test in sand.

4.2 Phase II: Quantitative Analysis

Although this phase has been labelled quantitative analysis, many results were still used to improve the testing procedure, such as during the introduction of pressure transducers. All tests have been done using the procedure outlined in Appendix C: Experimental Procedure for the Determination of Sweep Efficiencies.

4.2.1 Comparison of pulsed and non-pulsed experiments

The most fundamental tests compare pulsed and non-pulsed waterflood experiments, the goal of which is to identify fundamental performance differences. For this study, pulsed/non-pulsed results were compared using a series of four reservoir-depletion tests using glass beads. Reservoir-depletion tests refer to experiments where water is injected into the system until no oil was being recovered at the outflow. These experiments are used to determine the following three reservoir varibles:

1. **The rate of oil recovery.** Determined with sweep efficiency versus time graphs. The average rate is taken from the straight portion of the graph.

2. **The final sweep efficiency.** Determined with reservoir engineering plots (sweep efficiency versus pore volume injected). Refers to the final percentage of oil that can be recovered under the given conditions.

3. **The final flow rate.** Useful to compare flow rates at a given point in time. It does not consider the amount of oil being recovered.

The first two tests were done with 20–30 mesh glass beads (35.9% porosity), and the second two with finer, 30–40 glass beads (35.5% porosity). An attempt was made to use 40–50 glass beads, but air removal proved too difficult.

Table 4.2: Comparison of pulsed and non-pulsed experimental results.

	20–30 Beads (35.9% porosity)		*30–40 Beads (35.5% porosity)*	
	Non-Pulsed	Pulsed	Non-Pulsed	Pulsed
Average Oil Recovery Rate [ml/min]	13.3	5.1	9.5	2.6
Final Sweep Efficiency [%]	64	74	65	76
Final Flow Rate [ml/s]	4.9	12.3	3.8	11.7

Figure 4.1 is the sweep efficiency versus time graph, which as stated above, is useful for determining the rate of oil recovery. One may notice that the oil recovery slope for the pulsed

tests is significantly greater than that of the non-pulsed tests. For the 20–30 and 30–40 pulsed tests, the average oil recovery rate is 2.6 and 3.6 times greater, respectively.

Figure 4.2 is a reservoir engineering plot useful to determine the final sweep efficiency, which is the sweep efficiency at which no more oil is being recovered. The results taken from these charts are listed in Table 4.2. For the 20–30 and 30–40 tests, the final sweep efficiencies between pulsed and non-pulsed results differ by 10% and 11%, respectively.

Shown in Figure 4.3 are the flow rates. For the 20–30 tests, the maximum pulsed flow rate was over 2.5 times greater. For the 30–40 tests, the pulsed result was over 3 times greater. The flow rate variation seen in the pulsed results (in Figure 4.3) is due to pauses to refill the water reservoir.

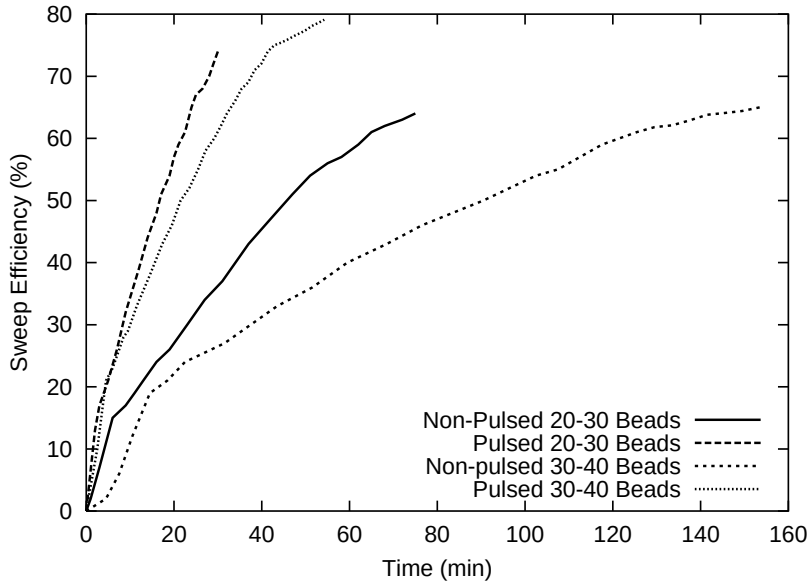

Figure 4.1: Sweep efficiency versus time for the reservoir-depletion experiments.

4.2.2 Comparison of pulsed experiments

The pulsed experiments are compared in a similar manner to non-pulsed/pulsed experiments. The important variables are the rate of oil recovery and the final sweep efficiency. Unfortunately, most of the pulsed experiments were not long enough to compare final sweep efficiencies, a problem discussed in Section 5.1.2. The inherent variablility of shorter experiments also makes the determination of average oil recovery rates difficult.

Figure 4.4 and Figure 4.5 summarize the experiments done for determining the effect of pulse pressure and pulse period. The results in Figure 4.4, which compare different pulse pressure, show very little variation in average oil recovery rates (rates vary between 12–14ml/min). There

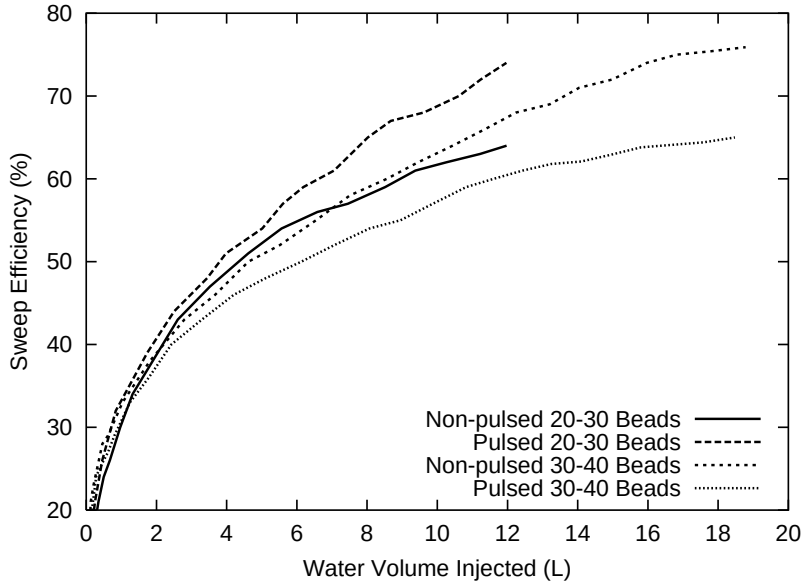

Figure 4.2: Sweep efficiency versus pore volume injected for the reservoir-depletion experiments.

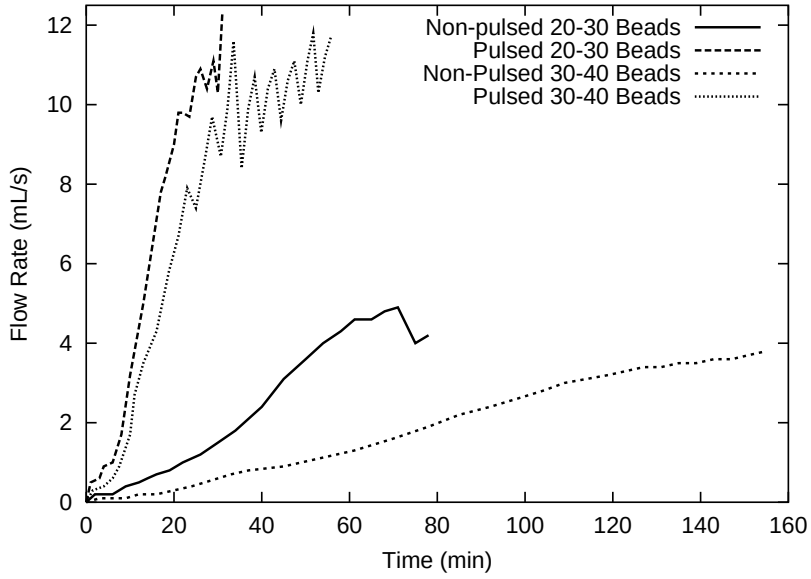

Figure 4.3: Flow rates for the reservoir-depletion experiments comparing pulsed and non-pulsed results.

is slightly more variation in the pulse period results, shown in Figure 4.5. The 0.75 second and 1.0 second results are all approximately 13–14ml/min, however the 1.2 second result is 8.6ml/min.

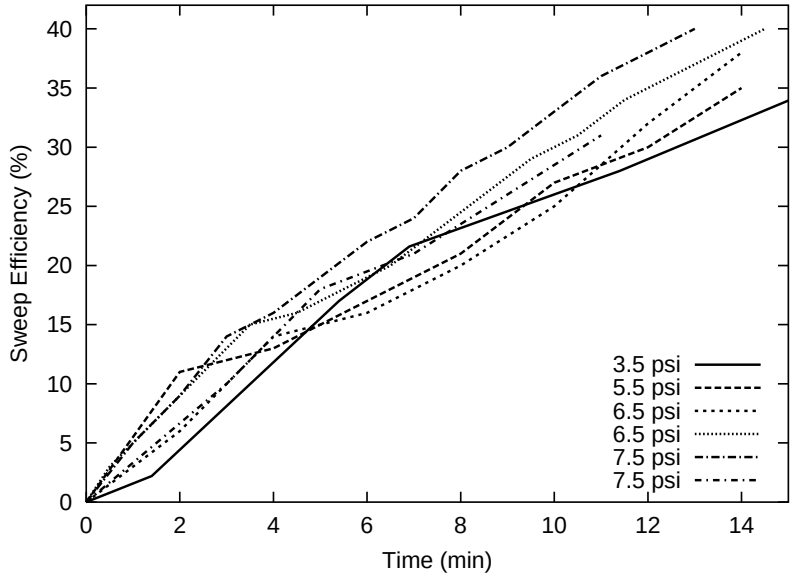

Figure 4.4: Variable pulse pressure tests. All other variables have been kept constant. 20–30 glass beads with 35.9% porosity.

At the end of the study, several pulsed, reservoir-depletion experiments were run. The tests are plotted in Figure 4.6 and the average oil recovery rates are listed in Table 4.3. Final reservoir sweep efficiencies are not listed because not all tests were done to full depletion. However, one can infer results relative to each test by looking at Figure 4.6.

Table 4.3: Comparison of pulsed experimental results.

Test Conditions	Average oil recovery rate [ml/min]
6.5psi pulse, 0.75s period, 20–30 beads	13.3
3.5psi pulse, 0.75s period, 20–30 beads	8.5
6.5psi pulse, 1.0s period, 20–30 beads	9.5
6.5psi pulse, 0.75s period, 30–40 beads	9.5

4.2.3 Emulsification

An interesting effect was observed when pulsing with the new CPS. It was noted that samples taken after water breakthrough had a “frothy” appearance, indicating that the oil formed an emul-

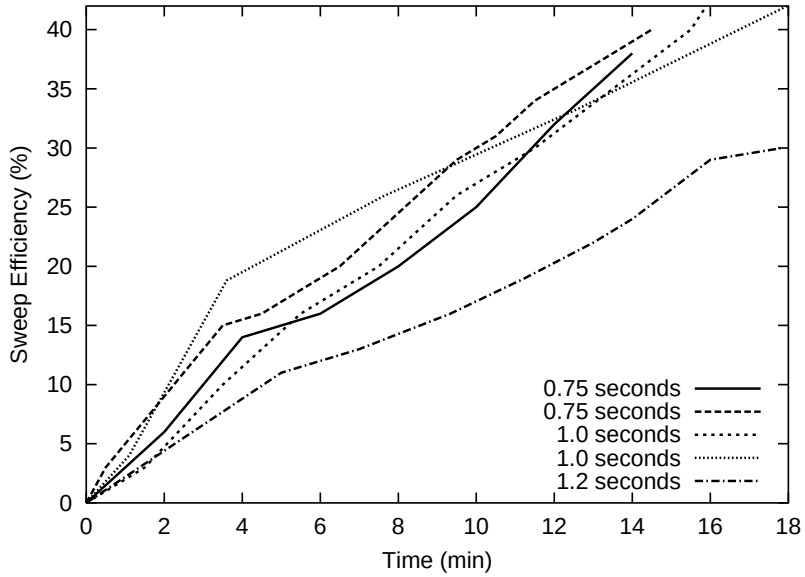

Figure 4.5: Variable pulse period tests. All other variables have been kept constant (35.9% porosity).

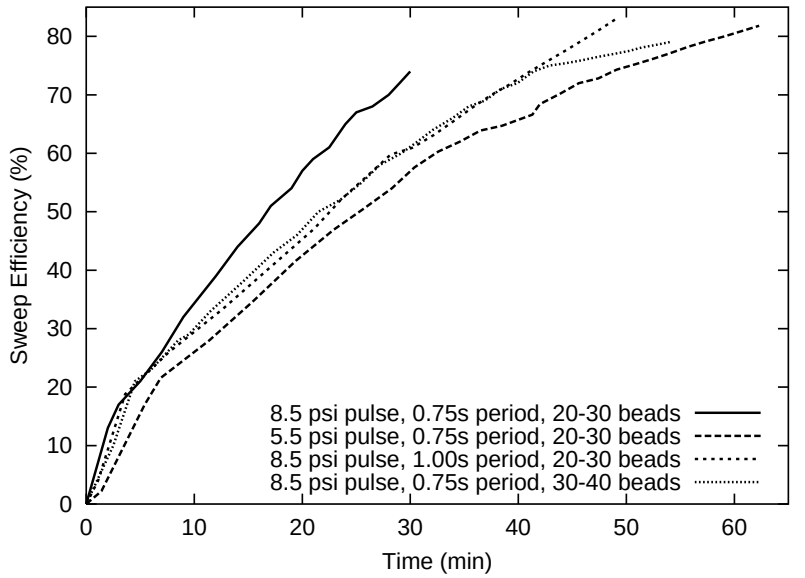

Figure 4.6: Variable pulse period and pulse pressure tests at a longer test duration. All other variables have been kept constant (35.8% porosity).

sion with water (Figure 4.7). The emulsion was formed when using light oils, was independent of the medium used, and was not attributable to residue on the medium.

Figure 4.7: Photo showing the emulsion produced by experiments. Samples to the left are clear and samples to the right are “frothy” in appearance, indicating emulsification.

Outflow observations for emulsified samples were always similar. Water breakthrough was not abrupt; rather it was first visible as tiny water droplets that increased in size until they filled the entire outflow tube. At the same time, the oil slowly changed in appearance from a clear fluid to a milky, frothy emulsion. This effect made the determination of water breakthrough difficult. Instead of a distinct frontal displacement front, there was a more gradual change, starting with tiny droplets of water that slowly got larger until they dominated flow.

Microscopic observation confirmed that this is an oil in water emulsion. It also revealed a consistent oil droplet size, similar to that of the pore throats.

Chapter 5

Discussion

The experimental limitations have had a direct effect on the results of this study, therefore this chapter starts there and is followed by a discussion of the results.

5.1 Limitations

There are three test limitations: the standard cell, the CPS water level problem, and the short-duration experiments. The last limitation is not due to equipment, but rather a testing methodology that was abandoned midway through the study.

5.1.1 The Standard Cell

The standard cell was designed primarily for visualization experiments, so it was not ideal for the study done here. The weakness of the felt seals and the flexibility of the Lucite^{TM} sides made higher stresses difficult because the cell would leak under high pressures. Furthermore, porosity calculations were difficult because the cell volume was not designed for making precision measurements. A machined metal cell would have been much easier to work with. However, the standard cell was not a significant limitation, and it should not have had an effect on the results. It is only mentioned so that future studies may consider that this cell is probably not the ideal piece of equipment.

5.1.2 Short-Duration Experiments

Early experiments were not long enough to adequately compare pulsed tests. Most lasted under 15 minutes, which was far less than later tests that lasted close to an hour. To observe why longer experiments were used, one can look at Figure 4.1. There is very little variation in the pulsed

results until well after 15 minutes. Similarly, it would have been difficult to draw conclusions from Figure 4.6 if the experiments had used the shorter duration.

The reason longer tests were not done earlier is due to a number of factors. First, the one-litre graduated cylinders necessary for accurate measurements were not available until later in the study. Secondly, the length of early experiments was limited by the CPS water reservoir. As discussed in the following section, refilling the CPS resulted in reservoir depressurization, which was not desirable because its effects were impossible to determine. However, when it was decided that conclusions were difficult to make at the current test duration, it was decided to start refilling the CPS. The initial results appeared rewarding, so the practice was continued and added to the experimental methodology. Unfortunately, the ultimate effect of refilling the water reservoir is still unknown.

5.1.3 CPS Water Level Changes

The CPS water level problem has two effects, it changes the pulse shape, and the reservoir depressurizes during refilling (introduced in Section 3.3). These limitations could both be eliminated by altering the CPS to maintain water levels. Many attempts were made to redesign the existing CPS, but none of the solutions worked or were practical (*i.e.* within budget). Since the completion of this lab study, a second CPS, which is based on the design presented here, has been made by a major oil company. This updated design overcomes the water level limitation, but the details of its operation have not been disclosed.

Reservoir Depressurization

The major CPS limitation is an inability to operate it for long periods of time without being refilled with water. This requires that the experiment be paused, causing the cell to lose pressure. The pressure change can be monitored indirectly by looking at flow rates*. For example, if one looks at the pulsed flow rates, such as the 30–40 result in Figure 4.3, there is a sawtooth pattern to the plot, which is visible on all experiments where water reservoir refilling was necessary (time is stopped during refilling). The flow rate decreases coincide with experimental pauses. It then takes up to two minutes of pulsing before the flow rate returns to its previous value. The effect of cell depressurization on final results is difficult to deduce, but it probably does not enhance the sweep efficiency of pulsing.

An interesting observation is that the flow variations seen in the lab are very similar to the pressure variations seen during workovers in the field. When doing a full-scale pulsing job, the pulsing is periodically stopped to allow the addition of annulus fluid. This results in a pressure

*The connection between flow rates and pressure was explained in Section 2.1

decrease around the wellbore, producing a graphical result very similar to that shown in Figure 4.3.

Pulse Shape Change

Before installation of the pressure transducers, there was concern that the pulse shape was varying widely during an experiment. The reason was again due to the water level changes, which made pressure increases necessary to compensate for additional air in the reservoir (Section 3.3). Therefore, an inflow transducer was installed that measured the pulse amplitude as three litres of water were removed (Figure 5.1). Three litres was chosen because it is the maximum amount of water removed before refilling.

There are several important observations that can be made from Figure 5.1. First, note that the pulse amplitudes are very similar, with the exception of part of the first pulse (Figure 5.1a). Second, the first pulse is sharper and more "bumpy" than the remaining pulses because there is no air to act as a damper. Accordingly, the last pulse is more rounded because the air volume in the reservoir is having a larger damping effect. Finally, the pulse lengths increase because of greater pressurization and depressurization times for the larger air volume.

Despite the changes in the pulse with time, the overall effect is not expected to be significant. The amplitude remains relatively constant and the length does not increase substantially (only 4 ms). Of far more concern is pausing the experiment, which was discussed earlier in this subsection. Furthermore, when the water level problem is solved, both errors will be eliminated.

What is interesting is that the pulse shape can be altered. If one wanted to determine the effect of pulse shape on pulsing, such as when dealing with the emulsification of light oils, this would be an interesting variable to experiment with. However, tests that require the pulse shape to remain constant naturally require the water level to remain fixed.

5.2 Comparison of Pulsed and Non-Pulsed Results

The current study has demonstrated for two-fluid phase systems what previous results had proved for one-fluid systems. That is, that pulsing results in much higher flow rates when compared to static waterfloods. As well, the current results have given a quantitative estimate of how much additional oil is recovered with pulsing and shown that pulsing results in much higher oil recovery rates.

The final sweep efficiency for all experiments is quite high (65–80%). This is due to the use of glass beads as the matrix; if sand had been used the sweep efficiency would have been lower. This is known from previous studies on Ottawa sand, which did not have the desired consistency for inclusion here.

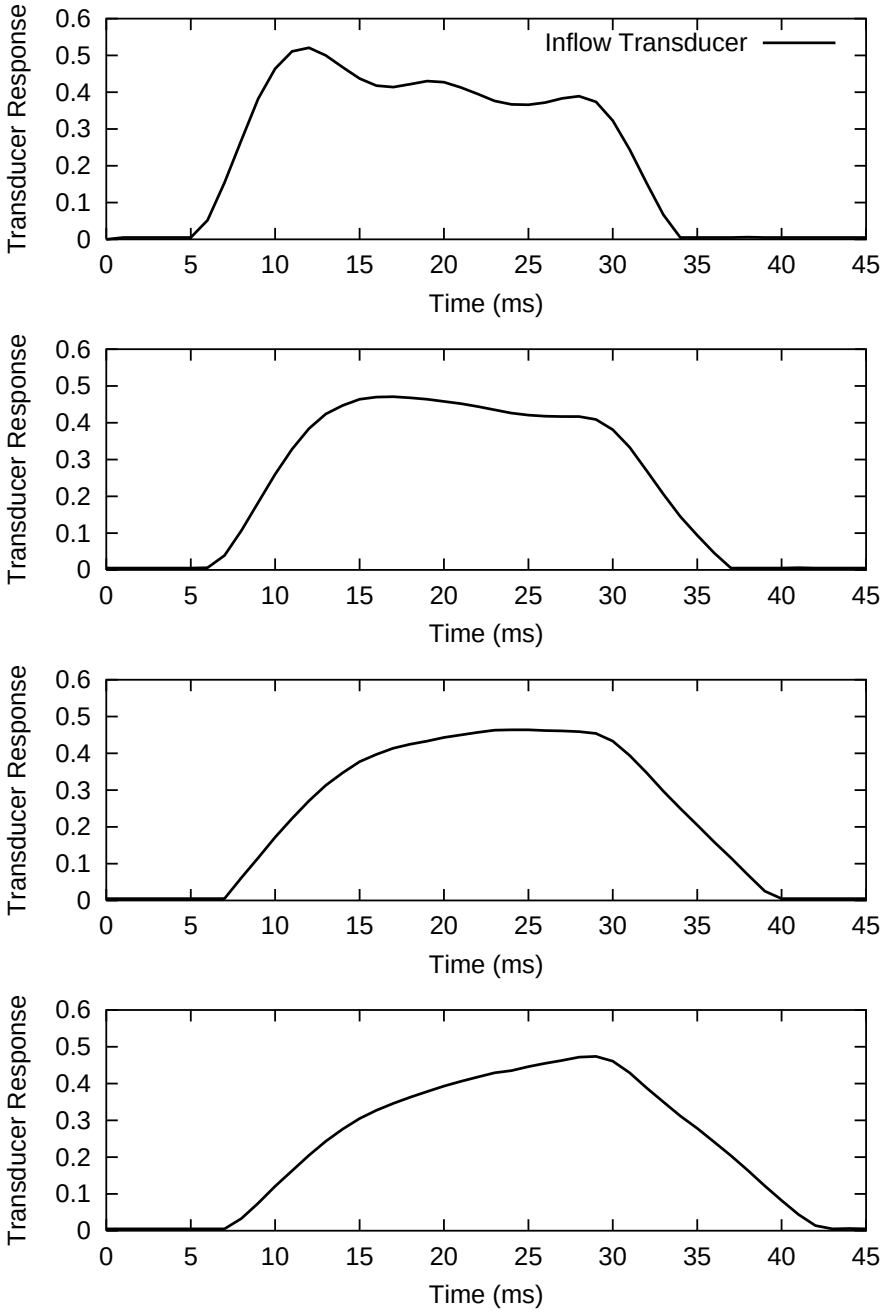

Figure 5.1: The change in pulse shape as three litres of water are pulsed out of the reservoir (for the problem background, see Figure 3.3). The y-axes have been named "Transducer Response" because the transducer was not properly configured for pressure readings. The lengths of each pulse are: a) 29ms; b) 30ms; c) 31ms; and d) 33ms. The pulse amplitude was approximately 5.5psi.

In Figure 4.1, one may notice that the slope of the graph changes with time. Initially, both graphs start out quite steeply, after which there is a change in slope. This is the point of water breakthrough. Furthermore, there appears to be a second, abrupt change in slope on the pulsed 30–40 plot, close to the end of the experiment. This may be because of the gradations on the 1-litre graduated cylinders. Because the oil concentrations being recovered from the outflow are so low, it makes their measurement difficult, leading to rounding errors. In reality, the change in slope may be more gradual, but it is difficult to say. The change in slope may also be due to the higher capillary pressures found between the smaller beads.

Finally, one can see that the slightly lower porosity of the 30–40 test resulted in slightly lower sweep efficiencies. It would have been desirable to compare final sweep efficiencies, but the 20–30 tests were not finished before they had to be discontinued due to to a container shortage.

5.3 Comparison of Pulsed Results

The comparison of pulsed results is made difficult by the short-duration limitation discussed in Section 5.1.2. Basically, any conclusions reached from the results shown in Figures 4.4 and 4.5 are tenuous at best. The plots are too short to determine final sweep efficiencies and they are also too short to get a reasonable estimate of oil recovery rates. When comparing the short-term results, it is best to focus on where the plots end, not the path that they take. This is because the long term plots display a large degree of variation at the beginning of a test and then start to separate later. All the long-term pulsed results have been compiled in Figure 4.6

5.3.1 Pulse Pressure

Looking at the long-term results in Figure 4.6, all that one can say is that there is a slight trend for decreasing sweep efficiencies with decreasing pulse pressure. Because there are only two plots to compare, it is impossible to make any other observations. The results shown in Figure 4.4 appear very similar, but closer examination reveals that there is definite separation at the ends of the plots. Therefore, pulse pressure has an effect on the results, but the exact relationship can not be determined.

5.3.2 Pulse Period/Frequency

Similar to the results for pulse pressure, not much can be said here that is conclusive. If one looks at Figure 4.6 again, it is apparent that there is decreasing sweep efficiency with decreasing pulse pressure. In Figure 4.5 there is not much variation between the 0.75 and 1.0 second tests, although there was a much larger variation in the long-term experiments. Interestingly, there is a very large difference between the 1.0 and 1.2 second results, which may indicate that sweep

efficiency decreases exponentially with decreasing period. This theory would naturally require more results for verification.

5.3.3 Porosity

An interesting effect is noticed when comparing the long-duration tests at different porosities. The lower porosity test, which uses 30–40 beads, shows an abrupt decline in sweep efficiency shortly after 40 minutes has passed. None of the 20–30 tests display this behaviour. This may be because of the smaller pore throats. Because the beads are circular and have been sieved, there is a characteristic pore throat size. Once the capillary forces of oil in these pore throats is greater than the force being exerted on them by the waterflood, the oil will stop flowing. More tests would be needed to verify this.

5.4 Emulsification

In experiments where an emulsion is formed, several interesting observations are noted. First, the emulsion forms only after water breakthrough; secondly, the water breakthrough is gradual; and lastly, a higher percentage of oil is displaced after breakthrough. This indicates that oil ganglia behind the main water displacement front are being mobilized, which is unusual due to the high capillary pressures that trap ganglia [27].

It is thought that the sharp pulses are forcing ganglia through pore openings, causing them to be “torn” apart, and they become smaller and smaller, forming tiny oil droplets that can move through the pore openings. The end result is an emulsion of oil droplets mixed in with the water at the outflow. This hypothesis is seemingly confirmed by microscopic observations that reveal a consistent oil droplet size, similar to pore throat sizes.

An important point to note is that the emulsion was not formed with hammer pulsing. This is thought to be because the pulse is not as sharp; therefore the dynamic forces at the pore scale are not great enough to tear the oil ganglia apart. However, more testing would be necessary to confirm this.

5.5 Application of Laboratory Results to the Field

It is difficult and sometimes impossible to apply results from the laboratory into the field. The variability of reservoir properties and the stage of application can have a large effect on the effectiveness of the technique. The result is an infinite number of possible situations which are difficult to account for. However, with simple experiments pulsing has proven to be an effective technique of removing more oil, most importantly by suppressing the formation of

viscous fingers. It also has the capability of pressurizing reservoirs, a desirable effect because it results in more oil outflow. Doubled flow rates and 10% more oil recovery than waterflooding would be very significant numbers in a field operation.

Based on this study, a valuable application would be in pulsing excitation wells to both pressurize the reservoir and enhance the sweep of the displacing fluid over a long-term period. It would also be valuable for short-term chemical injections, where mixing with the largest volume possible is desirable (Appendix F). Not surprisingly, both of these applications have already been tried and proven successful [5, 2, 28]. Pulsing has even proven valuable for removing mechanical skin, a type of formation damage, from the near-wellbore region in heavy-oil wells [28]. If the benefits of pulsing are readily visible in the field and laboratory, then perhaps the biggest challenge facing the technology is gaining acceptance within the oil industry.

Chapter 6

Conclusions and Recommendations

6.1 Conclusions

As with any new technology, the first studies are always exciting and very revealing. This project has been no exception, and there is still much to be learned and done experimentally. Overall, this thesis has been successful in establishing the lab methodologies and equipment that will be necessary for future studies. In fact, the CPS design has proven so successful that similar designs have been based on it and are now being used at a major oil corporation and a smaller EOR and monitoring company. However, these subsequent models have eliminated the water-level problem.

The conclusions taken from the two-fluid laboratory results are as follows:

- Pulsed tests had maximum flow rates 2.5–3 times higher, higher oil recovery rates (2.5–3.5 times higher), and final sweep efficiencies that were more than 10% greater than non-pulsed tests.
- Decreasing the porosity had the effect of lowering the sweep efficiencies. However, the 34.9% porosity results were not done until reservoir depletion, so it is difficult to quantitatively compare results.
- Longer pulsed tests (reservoir-depletion tests), suffered from a limitation of the Consistent Pulsing Source (CPS). They were periodically stopped to refill the water reservoir, resulting in reservoir depressurization and lower flow rates. The final effect of this is difficult to quantify without correcting the problem.
- The pulse shape changed slightly as water was removed from the reservoir. It is not expected that the change had any major effect on the results.

- The pulse pressure and period studies were limited by early tests, which did not have the necessary time duration. Both increasing pulse pressure and decreasing pulse period were found to increase the final sweep efficiency.

- An emulsion appears after water breakthrough when using the CPS on light oils (mineral oil). This may be the result of isolated oil ganglia being torn apart by the sharp pulses. The emulsion was not seen in earlier studies that used hammer pulsing, where the pulse was not as strong or sharp.

It is often difficult to apply results from the laboratory into the field. However, this study indicates that pressure pulsing as an enhanced oil recovery technique would be beneficial. Doubled or tripled oil recovery rates and 10% more oil recovery than waterflooding would be significant numbers in a field operation. A valuable application would be in pulsing excitation wells to both pressurize the reservoir and enhance the sweep of the displacing fluid over a long-term period. It would also be valuable for short-term chemical injections, where mixing with the largest volume possible is desirable. Both of these applications have already been tried in the field and met with success. It seems that the biggest challenge facing pulsing as an enhanced oil recovery method is gaining acceptance within the oil industry.

6.2 Recommendations for future laboratory work

- The current CPS design needs to be improved to accommodate water level changes within the reservoir. This would eliminate both the reservoir depressurization problem and the shift in pulse shape. Future studies are not recommended until the water-level problem is eliminated.

- More experiments should be done for the pulse period, pulse pressure studies. This is an important topic that the current study has only touched on. Further studies could verify and expand upon the few results presented here.

- Emulsification of light oils is a potentially very interesting project. More could be done to prove why it occurs and under what conditions.

- The current experimental cell was designed primarily for visualization studies. Future studies would be easier and more accurate with a specially-designed cell made from machined steel.

- When using light oils (paraffin oil), all future experiments should be done until reservoir depletion, which allows final sweep efficiencies to be compared. Crude oil experiments

should last until at least one pore volume has gone through the experimental cell. This will prevent experiments from being too short, minimizing variation.

- It is possible that variations in pulse shape have an effect on the results, particularly emulsification. A future study could be done to investigate this relationship.
- Finally, it would be interesting to try tests on consolidated core samples, not just in an experimental cell with sieved sand.

Bibliography

[1] B.C. Davidson, T.J.T. Spanos, and M.B. Dusseault. Laboratory experiments on pressure pulse flow enhancement in porous media. In *Proceedings of the* 8^{th} *CIM Regina Petroleum Society Technical Meeting*, Regina, Saskatchewan, October 1999.

[2] M.B. Dusseault, T.J.T. Spanos, and B.C. Davidson. A new workover tool: applications in CHOP wells. In *Proceedings of the* 50^{th} *CIM Petroleum Society Annual Technical Meeting*, Calgary, Alberta, June 1999.

[3] V. de la Cruz and T.J.T. Spanos. Thermomechanical coupling during seismic wave propagation in a porous medium. *Journal of Geophysical Research*, 94(B1):637–642, January 10th 1989.

[4] V. de la Cruz, P.N. Sahay, and T.J.T. Spanos. Thermodynamics of porous media. *Proceedings of the Royal Society of London*, 443(A):247–255, 1993.

[5] T.J.T. Spanos, B.C. Davidson, M.B. Dusseault, and M. Samaroo. Pressure pulsing at the reservoir scale: a new EOR approach. In *Proceedings of the* 50^{th} *CIM Petroleum Society Annual Technical Meeting*, Calgary, Alberta, June 1999.

[6] M.B. Geilikman, T.J.T. Spanos, and E. Nyland. Porosity diffusion in fluid-saturated media. *Tectonophysics*, 217:111–115, 1993.

[7] M. Samaroo. Pressure pulse enhancement: Report on the first reservoir scale experiment conducted by PE-Tech Inc. in Section 36 of Wascana Energy Inc.'s Morgan Field Lease. Master's thesis, Department of Civil Engineering, University of Waterloo, 1999.

[8] C.J. Hickey. Seismic wave propagation in porous media. Master's thesis, Department of Physics, University of Alberta, 1990.

[9] M.K. Hubbard. Darcy's law and field equations of flow of underground fluids. *American Institute of Mineralogy, Metallurgy, and Petroleum Engineering*, 207:222–239, 1956.

[10] S. Whitaker. The equations of motion in porous media. *Chemical Engineering Science*, 21:291–300, 1966.

[11] S. Whitaker. Advances in the theory of fluid motion in porous media. *Industrial and Engineering Chemistry Research*, 61:14–21, 1969.

[12] J.C. Slattery. Single phase fluid flow through porous media. *Journal of the American Institute for Chemical Engineering*, 15:866–872, 1969.

[13] R.C. Sharma and T.J.T. Spanos. Secondary and tertiary oil recovery. *University of Alberta, unpublished article*, October 1996.

[14] H.Y. Jennings, C.E. Johnson, and C.D. McAuliffe. A caustic waterflooding process for heavy oils. *Journal of Petroleum Technology*, pages 1344–1352, December 1974.

[15] D.J. Graue and C.E. Johnson. A field test of caustic flooding. *Journal of Petroleum Technology*, pages 1353–1358, December 1974.

[16] T.C. Boberg and R.B. Lantz. Calculation of the production rate of a thermally stimulated well. *Society of Petroleum Engineers Journal*, pages 1613–1623, December 1966.

[17] P.E. Baker. Effect of pressure and rate on steam zone development in steamflooding. *Society of Petroleum Engineers Journal*, pages 274–284, October 1973.

[18] T.R. Blevins and H.R. Billingsly. The ten-pattern steamflood, Kern River Field, California. *Journal of Petroleum Technology*, pages 1505–1514, December 1975.

[19] J.F. Lea, P.D. Anderson, and D.G. Anderson. Optimization of progressive cavity pump systems in the development of the Clearwater heavy oil reservoir. In *The Petroleum Society of CIM Technical Conference*, Calgary, Canada, 1987.

[20] D. Poon and K. Kisman. Non-Newtonian effects on the primary production of heavy oil reservoirs. In *The Petroleum Society of CIM and AOSTRA Technical Conference*, Banff, Canada, 1991.

[21] F.I. Stalkup. Status of miscible displacement. *Journal of Petroleum Technology*, April 1983.

[22] D. Morel. *Miscible Gas Flooding, in Basic Concepts in Enhanced Oil Recovery Processes*. Elesevier, 1991. Edited by M. Baviere.

[23] J.A. Boon. Chemistry in enhanced oil recovery - an overview. *Journal of Canadian Petroleum Technology*, January-February 1984.

[24] M.B. Dusseault. Canadian heavy oil experience using cold production. In *Proceedings of the Trinidad and Tobago Biennial SPE Conference*, Port-of-Spain, Trinidad, November 1998. CD-ROM available from SPE Trinidad and Tobago Section.

[25] A.C. Woynillowicz. Pressure pulsing for aquifer remediation. Undergraduate thesis, Department of Geological Engineering, University of Waterloo, 2000.

[26] F.W. Cole. *Reservoir Engineering Manual*. Gulf Publishing Company, 1969.

[27] V. de la Cruz and T.J.T. Spanos. Mobilization of oil ganglia. *AlChE Journal*, 29(5):854–858, September 1983.

[28] M.B. Dusseault, B.C. Davidson, and T.J.T. Spanos. Removing mechanical skin in heavy oil wells. In *Proceedings of the 2000 SPE International Symposium on Formation Damage*, Lafayette, Louisiana, February 2000.

Appendix A

The Consistent Pulsing Source (CPS)

There are two CPS designs, the piston and the compressed-gas models. The first design was not very successful and was abandoned, the second was used for most lab results and a variation of it is now used in the field.

A.1 Details of the piston CPS design

The first CPS was based on a piston design at the University of Waterloo. The construction was limited to two main pieces, a piston and a cylinder (Figure A.1). Placed at the bottom of the cylinder were inlet and outlet ports with one-way flow valves (check valves) installed. To operate the CPS, the piston was pulled up by hand and then dropped. As the piston was raised, air would enter the cylinder through the inflow. On the downstroke, all the water would be expelled through the outflow, generating a pulse. This design required two water reservoirs, one to place a consistent pressure on the cell, and another to supply the cylinder with water.

The piston design had advantages. It closely modelled what is used in the heavy oil industry, it moved very smoothly, and a valve in the piston prevented air from entering the outflow. Unfortunately, the design also had many disadvantages, which are listed here:

1. The design depended on check valves. These were found to significantly lower flow, reducing the effectiveness of the pulse. In retrospect, any small design that relies on check valves and extremely fast timing is going to encounter difficulties.

2. The Teflon split rings, which were used to prevent water flow around the piston, were leaky. This was expected, but it was not expected that it would create a large mess every time an experiment was run, especially if blue dye was being used.

3. The tolerances between the piston and cylinder were very tight, making it difficult to machine the parts without warping them. The pulser was extremely difficult to work with in

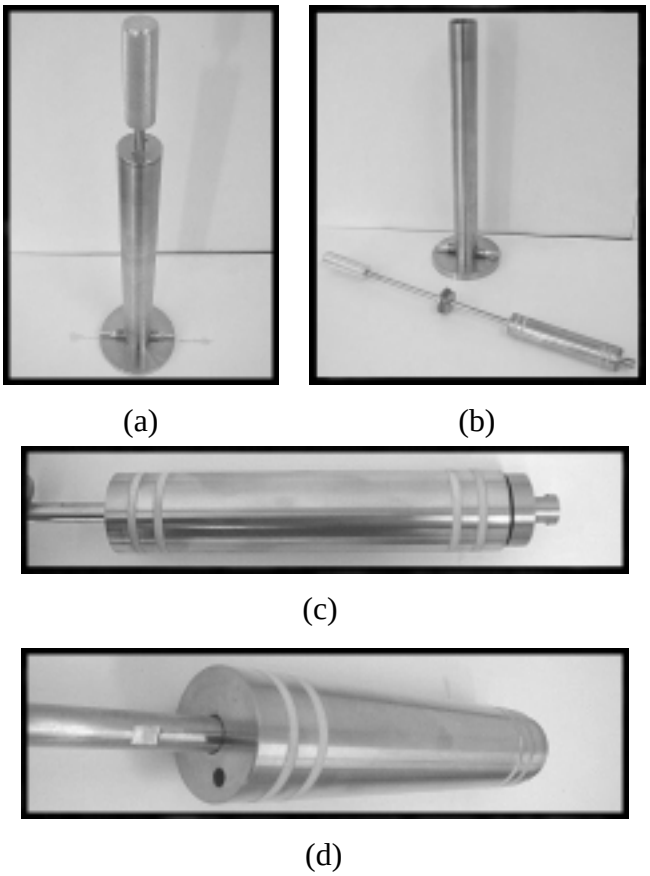

(a) (b)

(c)

(d)

Figure A.1: The piston CPS without check-valves attached a) shown together, and b) disassembled. c) Close-up of the piston showing the valve in an open position. d) Piston close-up showing the air hole; a second one was added later.

the machine shop.

4. Because the pulse was manually operated, it was difficult to control variables such as frequency and pulse duration.

All of these problems may have been overcome or minimized with time, however a second, more innovative CPS was designed which seemed to answer many of the problems.

A.2 Details of the compressed-air CPS design

The piston design failed as a useful tool because it was heavy, not automated, incapable of controlling pulse duration, difficult to use, and time-consuming to create. The second design took a completely different approach.

A.2.1 Design and Operation

The compressed-gas design is quite simple; it uses two solenoid valves, a square wave generator, and a relay. The solenoid valves, which are electronically controlled valves, are used to pressure and depressurize the reservoir. The relay switches the electric current between the two solenoids, and the square-wave generator is used to toggle the relay.

With reference to Figure A.3, the operation can be explained as follows. Solenoid 1 connects the reservoir to the atmosphere; Solenoid 2 connects the reservoir to the pressurized gas. When the CPS is started, Solenoid 1 is open and Solenoid 2 is closed, therefore the reservoir pressure is atmospheric. During a pulse, Solenoid 1 closes and Solenoid 2 is opened, pressurizing the reservoir. To turn off the pulse, Solenoid 2 is closed and Solenoid 1 is opened. In this fashion, only one solenoid is on at any given time. Switching between the two valves is carried out by a simple relay that is toggled by a square-waveform generator.

The large accumulator (visible in Figure A.4) was included to overcome a low flow coefficient through the pressure regulator. A longer period between pulses resulted in stronger pulses because pressure was allowed to build up for a longer period of time. By including the accumulator, or air-ballast reservoir, before the solenoids, the pressurization time was decreased significantly. It may not have been necessary for experiments using the compressed-gas line, but it was essential when using a nitrogen tank.

It was found that a relatively small water level change could have a large effect on the pressure pulse. This was because the larger volume of air in the cylinder resulted in longer pressurization times, which decreased the pulse pressure by 1 psi for every liter of water leaving the reservoir. Many direct solutions to this problem were attempted, but they all relied on perfectly synchronous solenoid valves. Unfortunately, the valves were not toggled immediately, rather

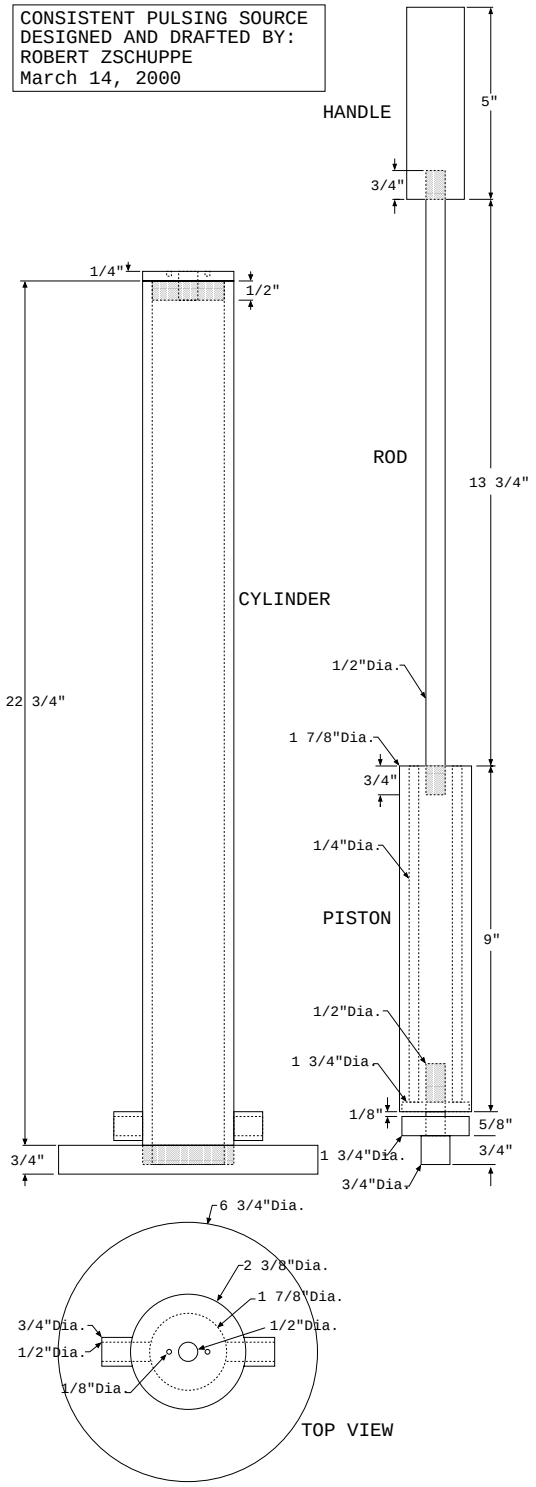

Figure A.2: Plans for the piston CPS.

there was a slight delay as the waveform of the 60Hz electrical source reached its maximum slope. The consequence was slightly asynchronous solenoid valves. Therefore, an indirect solution was used to compensate. The air pressure supplied to the water reservoir was steadily increased, giving a consistent pulse pressure, frequency, and period. The disadvantage was that once three liters of water had been used, the increase in air pressure could no longer compensate for the longer pressurization times. At this point, the experiment was briefly paused and the water reservoir refilled. This affected the final results, because pausing the experiment caused the cell to lose pressure, which in turn resulted in lower flow rates.

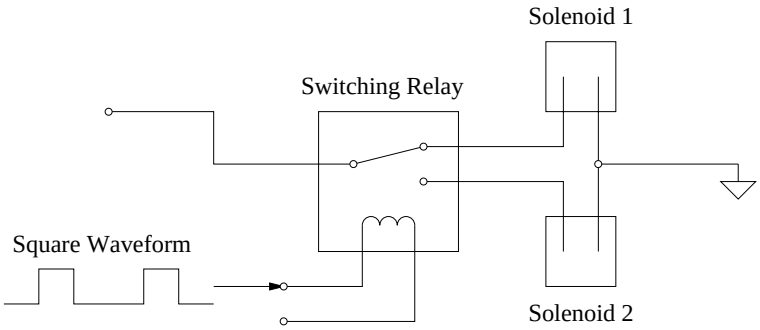

Figure A.3: Schematic diagram of the CPS relay system. The square wave pulse switches the relay, which in turn alternates power between the two solenoid valves. The valves are connected to the compressed air and the water reservoir.

Figure A.4: The compressed-gas CPS. The two tanks are the water reservoir and air accumulator. The two solenoid valves control air pressure in the water reservoir. Finally, there is a square-wave generator with a relay box on top of it, this controls the solenoid valves.

Table A.1: Solenoid Valve Specifications

ASCO Red-Hat Solenoid Valve *closed when current is off	
Cat #:	8222D2LT
Volts:	120/60 V
Watts:	16.7 W
Media:	Liquid Nitrogen
Pipe:	1/2 inch
Orifice:	5/8 inch
Pressure:	125 psi

Appendix B

Consistent Pulsing Source (CPS) Operation

The compressed-gas CPS is straightforward to operate once the components have been put together. All of the major parts are shown assembled in Figure B.1. The only parts missing are the air accumulator and wave generator, which are pictured in Appendix A, Figure A.4.

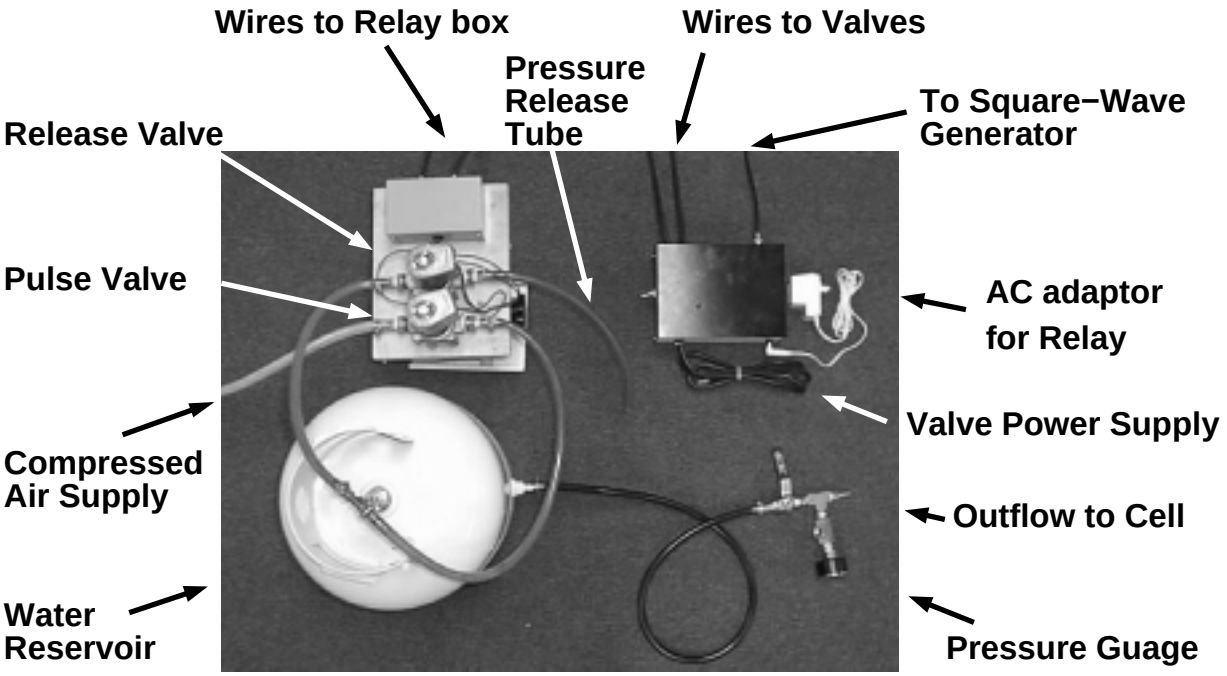

Figure B.1: An overview of the CPS labelling all the major parts. The air accumulator and square-wave generator are not pictured.

B.1 CPS Components

The components that have a bearing on the CPS operation are described here.

B.1.1 Air Accumulator

The air accumulator is not technically a part of the CPS, nor is it always necessary. It is only used when the air flow is insufficient to pressurize the CPS between pulses. For example, the original experiments required an accumulator because they used a pressure regulator with a very low flow coefficient (the regulator was used with a portable nitrogen tank). Later experiments did not require the accumulator because they used the air supply in a well-equipped research building.

To determine whether a larger accumulator is necessary, a pressure gauge can be installed on the air-supply line to monitor consistency. If a pressure gauge is not available, a rough estimate can be made. Run the CPS with a short period (0.6 seconds), placing the outflow in a sink. After 10 seconds, turn the CPS off. If air is still whistling into the air accumulator, a larger accumulator is necessary. Note that it is a better idea to buy the pressure gauge, because if a test is run with an insufficient accumulator, the experiment will have to be redone.

B.1.2 Relay Box

The relay box schematic, detailing the exact components used, is shown in Figure B.2.

B.1.3 PC Automation

The CPS was briefly set up with PC automation using Lab-VIEW. This controlled the relay box (*i.e.* period and pulse length), timing, as well as monitoring the inflow and outflow with pressure transducers (the outflow transducer produced erroneous results). The automated system simplified the laboratory procedure, but was used mainly for the transducers.

B.2 CPS Usage Procedure

1. Assemble the CPS as shown in Figure B.1.
2. Calibrate the square-wave generator with an oscilloscope (unless using a PC-automated system).
3. Turn the air-supply source on. The solenoid valves are closed when they are off, so the air supply will not pressurize the water reservoir.

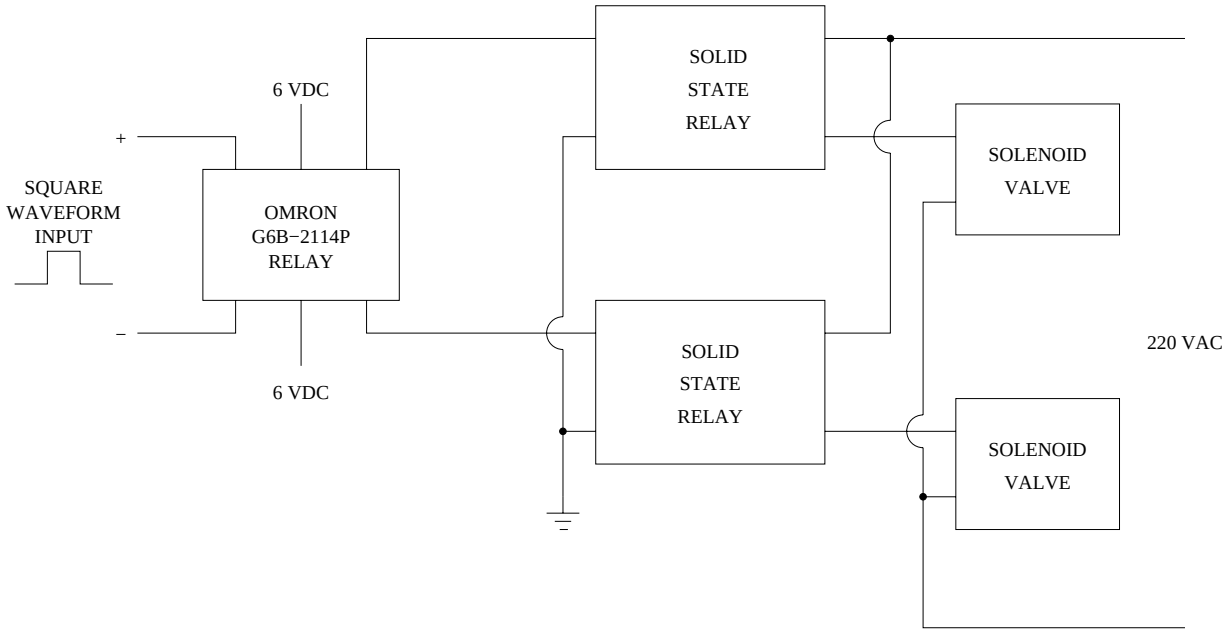

Figure B.2: Relay box schematic. The solid state relays were only used to reduce noise. The exact solenoid valve specifications are given in Table A.2.1

4. Run a pulse pressure test:
   (a) Shut the valve immediately before the inflow of the experimental cell.
   (b) Start the CPS by turning the relay box on.
   (c) Ensure the solenoid valves have been wired correctly (Is there a short pulse and long pause, or has it been mis-wired?).
   (d) Calibrate the air-supply pressure to give the desired pulse pressure (remember that the pulse pressure is the pressure above static). Note that the pulse pressures monitored at the gauge have been shown to be quite accurate, despite the difficulty of reading from a rapidly-moving needle. If the system is PC automated, monitor the pulse shape as well.
   (e) Shut off the CPS (at the relay box).
5. Turn the CPS on (at the relay box).
6. At the same time, start the timer and open the valve located before the inflow of the experimental cell. If using PC automation, start the CPS and open the inflow valve at the same time.
7. Turn the CPS and air-supply off once the test is done.

B.3 Typical CPS Settings

The typical CPS settings at this point are rather arbitrary. The standard test conditions are a 0.25s pulse length, a 0.75s period, and a 5.5psi pulse. The pulse length has never been altered, however the periods and pressures have been varied between 0.65–1.2s and 2.5–7.5psi, respectively.

Appendix C

Experimental Procedure for the Determination of Sweep Efficiencies

C.1 Purpose

The experimental purpose is to compare the sweep efficiencies under pressure pulsed and non-pulsed conditions.

C.2 Corrections

The purpose of the corrections is to subtract the influence of tubing and reservoir volumes on either side of the cell volume (Figure C.1). This is because the final results should only test the porous medium, which is in $V3$ in Figure C.1. All corrections take into account that the reservoirs and tubing are initially filled with oil (Volumes 1_{in}, 1_{out}, 2_{in},and 2_{out}).

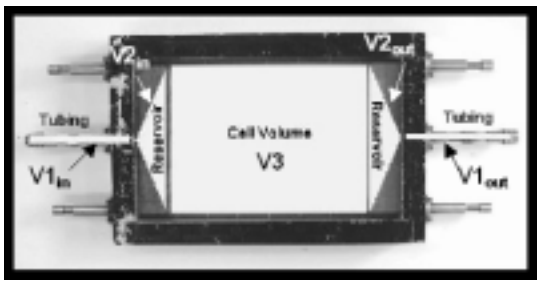

Figure C.1: The standard cell with white-filled rectangles and triangles to show where fluid volumes are stored in the cell. Volumes 1 and 2 ($V1$ and $V2$) are for the tubing and reservoir at the inflow and outflow, respectively. Corrections are used to subtract the influence of $V1$ and $V2$ from the final results.

C.2.1 Time Correction

The test should be started when the waterflood enters the sand, not when the waterflood enters the experimental cell. Because only the second case can be measured, a time correction is used to account for the volume filled by the waterflood before reaching the sand. To apply the correction, volumes 1_{in} and 2_{in} are divided by the volumetric flow rate to estimate the actual start time. This time is then subtracted from the measured time to give the corrected time (Equation C.1).

$$t_{corrected} = t_{actual} - \left[\frac{V1_{in} + V2_{in}}{Q}\right] \tag{C.1}$$

where $t_{corrected}$ is the corrected time, t_{actual} is the measured time, $V1_{in}$ is the the volume of the tubing, $V2_{in}$ is the volume of the bottom reservoir, and Q is the volumetric flow rate.

C.2.2 Inflow Correction

The inflow correction is related to the time correction. Because the test does not actually start until the waterflood reaches the sand, the volume leading to the sand must be subtracted from the outflow volume (Equation C.2). This assumes that water completely fills the bottom reservoir and tubing (Volumes 1_{in} and 2_{in}).

$$V_{outflow} = V_{outflow} - V1_{in} - V2_{in} \tag{C.2}$$

where $V_{outflow}$ is the cumulative volume of the outflow, $V1_{in}$ is the volume of the tubing, and $V2_{in}$ is the volume of the bottom reservoir.

C.2.3 Outflow Correction

Similar to the inflow correction, an outflow correction is made to account for the concentration of oil and water in the upper reservoir and tubing (Volumes 1_{out} and 2_{out}). This correction is applied to the actual volume of oil displaced with time. The outflow correction is more complicated than the inflow correction because the ratio of oil to water in the reservoir and tubing changes with time. To make the correction, fluid concentrations in volumes 1_{out} and 2_{out} are assumed to mirror the actual outflow concentrations. The concentration of water in the outflow, which is measured every 60 seconds, is used to estimate the concentration of water in the reservoir and tubing over the same time period (Equation C.3).

$$V_{oil\ outflow} = V_{oil\ outflow} - \%water \times \left(V1_{out} + V2_{out}\right) \tag{C.3}$$

where $V_{oil\_outflow}$ is the cumulative volume of the oil outflow, $\%water$ is the percentage of water in the outflow, $V1_{out}$ is the volume of the tubing, and $V2_{out}$ is the volume of the top reservoir.

C.3 Preparation and Test Procedure

1. Assemble the experimental cell, leaving the top assembly off.
2. Place the bottom of the cell in a large clamp to hold it upright. Use C-clamps to attach the pneumatic vibrator to the side of the cell. The cell should be in the orientation seen in Figure C.2.
3. Connect the water tube to the bottom assembly and fill the cell halfway with water (Figure C.2 shows the cylindrical flask used for adding water). Remove all air from the bottom tubing and reservoir.
4. Start the vibrator and add sand until it is 7-8cm from the top of the Lucite, ensuring that no air is trapped in the sand. Remember to measure the mass of the sand, this is necessary for porosity determinations. Note that some water will need to be removed while packing. Make sure the water level never drops below the level of the sand.
5. Run water through the top assembly to get it wet, this helps prevent trapped air. Attach the top assembly, brass fittings, and tubing. Do not excessively tighten the bolts.
6. By tightening the reservoir, apply enough stress to the sand so that it does not move when pulsed. Do not apply a large amount of stress because the bolts used to attach the top assembly may lock, strip, or break. Calculate the volume of the cell.
7. Calculate the porosity using Equation C.4.

$$Porosity = \frac{Mass\ of\ medium/Medium\ density}{Cell\ volume} \tag{C.4}$$

8. By raising the water reservoir, add water until it is at the very end of the upper tubing.
9. Attach the paraffin oil tubing to the top assembly tubing. The paraffin oil reservoir should be at least a meter above the cell. The water reservoir should not be lower than the top of the experimental cell.
10. Allow the paraffin oil to flood the cell.
11. The paraffin oil flooding front will not be visible as it passes though the cell. However, it will be visible in the tubing. Shut the bottom valve as soon as the front reaches the end of the bottom assembly tubing.
12. Disconnect the water tubing at the bottom. Attach the coloured water reservoir to the bottom.

13. Disconnect the paraffin oil tubing from the top. Place the end of the short span of tubing in the pole clamp (Figure C.2). It is useful to have a stand to collect oil from the outflow when the test is started.

14. Elevate the water reservoir until the desired head difference between the top of the reservoir and the outflow tube is reached.

15. Get ready to start the test: get the clock ready, have 10-20 beakers on hand, note-pad outlining the sample times. If pulsing: use either a mallet or the consistent pulsing source (if using a mallet, be sure to pulse as close to the inflow as possible),

16. Open the top and bottom valves and start the test. Collect the outflow in a beaker.

17. Change the beaker for each time interval. Place the used beakers in an ordered row.

18. Continue the test for the desired length of time and then shut the valves.

19. Measure the amount of water and oil in each of the beakers with a graduated cylinder.

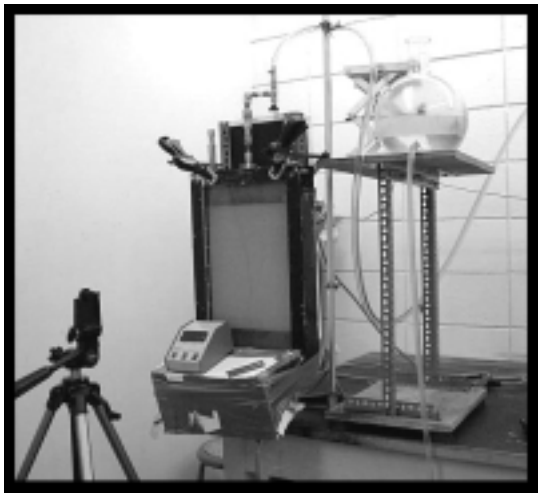

Figure C.2: Experimental setup for vertical tests. This picture shows the orientation of the cell, the camera tripod, the timer, and the lighting system that is clamped to the back of the cell. Please note that in this study almost all experiments used a horizontal orientation.

Appendix D

Experimental Cell Usage

This section explains how to assemble and disassemble the three experimental cells at the University of Alberta. It is highly recommended that the instructions be followed.

D.1 The Standard Cell

The standard cell has movable reservoirs capable of applying stress to the matrix. The cell is not used for heavy oil because it would be difficult to clean and requires significantly more oil than the low-volume cell (Section D.3).

D.1.1 Common Problems

Air entering the sample. Probably trapped air from the top or bottom reservoir assemblies. Ensure that all air is out of both reservoirs.

D.1.2 Assembling and Packing the Cell

1. Put the Lucite^{TM} plates, bottom assembly, and side assembly together, applying vacuum grease where appropriate. Tighten the bolts with a standard Allen (hex-) key.

2. Attach the cell to a water reservoir and fill the cell halfway with water.

3. Be careful. Air easily gets trapped in the bottom assembly. Screw the bottom assembly up and down several times to get rid of trapped air. Try pulsing at the same time.

4. When the air has been removed, ensure that the top of the bottom reservoir is aligned with the black line. This allows the bottom reservoir to be moved up or down if the need arises.

5. Attach the vibrator and start it.

6. Start pouring sand in with a small beaker. Continue until it is approximately at the level the top reservoir would be at when installed.

7. Insert the top reservoir assembly, ensuring that it is at its minimum extension.

8. Screw the top reservoir assembly in. Screws should be done very tightly, as before.

9. Add enough water so that it is coming out of the top assembly tube.

10. Again, be very careful. Even if the cell is reasonably level, you can still get air trapped in the top reservoir.

11. Once the air is out, extend the reservoir assembly so that it compresses the sand. If porosity measurements are needed, it will be necessary to control the distance between reservoirs.

12. If saturating the cell with paraffin oil, attach the paraffin oil reservoir tube to the top of the cell (remember: paraffin oil is less dense than water). Be sure that no air enters the system.

13. Ensure that the paraffin oil reservoir is located high above the cell. The water reservoir should be located just a little higher than the cell.

14. The paraffin oil will displace the water. The displacement front may not be visible across the cell (depending on media), but it will be visible when it enters the tubing. Stop the flow in the water tube, not the paraffin tube. This keeps the cell under pressure.

D.1.3 Cleaning the Cell

1. Remove the top assembly.

2. Turn the cell upside down over a garbage pail and open the bottom valve. The contents should slide out.

3. Clean the cell in the sink with dish soap and hot water. Removal of the bottom assembly is not necessary.

4. If the bottom assembly is not being removed, remember that a lot of oil can be trapped in the reservoir and held in by the screen. Place the cell on its end and let all the oil drain out (and then clean it again). Or remove the oil by attaching the bottom assembly to a water tap and letting hot water flow through the cell for several minutes. This will remove most of the oil.

Figure D.1: The large experimental cell.

D.2 The Large (Demonstration) Cell

This cell is used primarily for demonstration purposes.

D.2.1 Common Problems

All the glass beads can not be packed back in. The glass beads must be packed tighter. Insert the top assembly and use it to compress the glass beads. It is important to make sure the C-clamps are on, otherwise the sides will bow out. When finished, remove the top assembly and add more beads.

The sides are bowing out. The sides will always bow out a bit, but it is worse when the C-clamps have been forgotten. Unfortunately, this is difficult to remedy without removing the beads.

It is leaking from the top. There is a butt-joint near the top of one of the Lucite^{TM} sides that leaks. It can not be stopped without fixing the joint.

There is a little bit leaking from the bottom. There is almost always a little bit leaking from the bottom. Leakage can be minimized by tightening the bolts as hard as possible (but be

easy on the 4 Allen-key bolts). Make sure neither the orange rubber spacer, the O-ring, or the vacuum grease has been forgotten.

D.2.2 Assembling and Packing the Cell

1. Apply a thin layer of vacuum grease around the large O-ring at the bottom of the cell. Install the bottom assembly, making sure to place the orange rubber spacer between the assembly and the Lucite^{TM} cell.

2. Secure the bottom assembly using the two Allen-key bolts. Insert the remaining 14 bolts and tighten.

3. Apply the C-clamp to the bottom (visible in Figure D.1). This will help prevent the beads from warping the sides.

4. Place the copper screen above the bottom assembly reservoir to prevent the glass beads from entering.

5. Tilt the cell 45° and slowly roll the beads in. Try to prevent beads from getting under the copper screen (it does not matter if a a few get under it).

6. After putting several inches of beads in, tap the sides of the cell with the rubber mallet to increase the packing density. Repeat until the cell is full.

7. Once the cell is full, there may be left-over beads (see common problems).

8. Place the copper screen on top of the beads. The height of the beads should be high enough that there is not quite enough room for the reservoir to fit.

9. The orange rubber seal is not necessary for the top assembly, the O-ring alone should be enough. Do not forget to smear vacuum grease around the O-ring.

10. Before installing the top assembly, ensure that the reservoir has been screwed to it's minimum extension.

11. Place the copper screen on top of the glass beads. Do not worry about getting the top of the beads perfectly flat, the next couple steps will take care of that.

12. The beads can be compressed further by banging the Lucite^{TM} walls with a rubber mallet while pressing down on the top assembly. Make sure the C-clamp is in place (see common problems).

13. Secure the top assembly to the cell. Unlike the bottom, the 14 bolts do not need to be tightened to the point of failure. Nor does the orange, rubber spacer need to be used.

14. Tighten the C-clamp so that the top does not look warped.

15. Re-tighten the 14 bolts.

16. The beads can be compressed further by screwing the reservoir down while banging on the side. Be careful not to expand the sides of the cell.

17. Flood with glycerin.

NOTE: the cell will leak at a Lucite^{TM} butt-joint near the top of the cell. This joint can be found on only one side of the cell and it is covered by the top assembly. When the cell has been assembled, it is best to angle it so that the joint does not leak.

D.2.3 Disassembling the Cell

1. Drain the cell overnight by placing the glycerin reservoir lower than the cell. The cell can be drained faster by elevating it.

2. After all of the recoverable glycerin has been removed, close the bottom tube (which is attached to the glycerin reservoir).

3. Remove the top assembly (if it hasn't already been removed), the O-ring and the copper screen. Clean the top of the Lucite^{TM} cell.

4. Place duct-tape across the top 3/4 of the Lucite^{TM} cell.

5. Get one of the large plastic containers to empty the beads into, preferably one with high sides.

6. Slowly angle the cell and let the beads roll into the container. You may want to hold the container directly under the cell because the beads will bounce.

7. After removing all the beads, take the duct-tape off and remove the bottom copper screen.

8. Sweep all the beads off the floor that bounced out.

D.2.4 Cleaning the Cell

1. Attach a water hose to the bottom assembly of the large cell. Rotate the cell so that water flows out of the cell.

2. Route hot water through the hose and let the water run though the cell. The use of a plastic container to collect the water and duct-tape to block the top of the cell would be recommended.

3. Clean the top assembly using hot water. Soap can be used, but it may leave a residue and it is not absolutely necessary.

4. The glass beads can be cleaned by repeatedly filling and emptying the plastic container with hot water while agitating the beads. Empty the container by either pouring into a sieve (fast, but dangerous and sometimes difficult) or using a siphon tube (slower, may still want to use a sieve).

D.3 The Low-Volume Cell

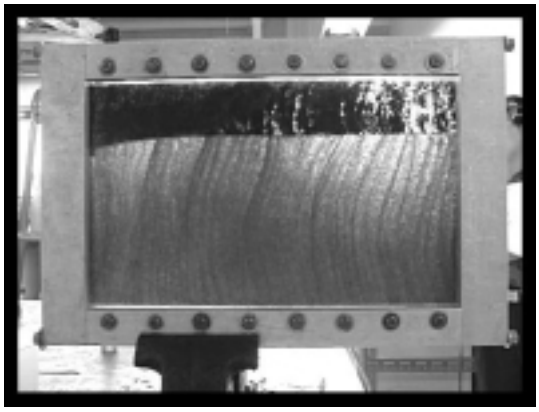

Figure D.2: The low-volume experimental cell.

The low-volume cell does not have the capability to apply stress to the ends of the cell. However, it is easy to clean and does not hold very much (hence the name low-volume cell).

D.3.1 Common Problems

It is leaking at the bottom. Two possible sources: either vacuum grease was not properly applied to the O-ring, or the screws in the Lucite^{TM} need to be tightened (the latter is generally the culprit).

It is leaking from the sides. The vacuum grease has formed an incomplete seal between the spacers, or the bolts may just require tightening.

The Lucite^{TM} spacers or metal strips do not fit correctly. Make sure they are in the correct orientation. There is only one specific way for everything to fit together.

D.3.2 Assembling and Packing the Cell

1. Put vacuum grease on both sides of the Lucite^{TM} spacers.
2. Lay the Lucite^{TM} parts together, making sure the spacers and sides are in the correct orientation (otherwise you will never get it together). There should be an A and B on the sides to guide you (one of the spacers had to be replaced and is no longer labelled).
3. Put the cylindrical metal dowels in first, this ensures that the parts are fitting together correctly. Next, screw the bolts in, these will have to be re-tightened later.
4. Get the metal sides and the two metal strips. Put the bolts through and tighten. Make sure the bolts are extremely tight.
5. The screws in the Lucite^{TM} will have to be re-tightened at this point.
6. Put one of the two assemblies on the end. Remember to cover the O-ring with vacuum grease. Do not forget the metal screen.
7. Tighten the four Allen-key bolts very tightly.
8. Place the cell upright in a vice. Attach the bottom assembly to a water reservoir and fill halfway with water.
9. Wait at least 5 minutes to see if it leaks. If it leaks, see common problems section.
10. Attach the vibrator with the C-clamps. Start the vibrator. Hope that it does not suddenly start to leak.
11. Add sand to the cell. Fill all the way up to the top. Make sure the sand is always saturated in water.
12. Clean the top of the cell and then install the top assembly (without forgetting the O-ring, vacuum grease, or metal screen).
13. Add more water to the cell.
14. When using the metal spacers (which apply a stress to the cell), both the top and bottom assemblies will have to be removed to insert them.

Appendix E

LNAPL Contaminant Lab

The Light, Non-Aqueous Phase Liquid (LNAPL) experiment was run on March 15^{th}, 2000. It was followed by a series of similar environmental labs by a University of Alberta graduate student.

E.1 Purpose

To observe the effects of a pressure pulsing assisted waterflood in a system where a LNAPL saturates a zone immediately above water.

E.2 Preparation

The low-volume experimental cell (Appendix D.3) was packed with two layers that were added simultaneously during vibro-densification. A contaminant in Ottawa sand formed the upper layer, and the lower portion consisted of water in finer, well-graded sand. The inflow/outflow ports were placed near top to limit the majority of the pulsing to the Ottawa sand and the upper part of the lower layer. Pulsing in the field would also be done largely in the contaminant zone.

Air was accidentally allowed into the system on the exit side. Because air compresses quite easily, it reduces the effectiveness of pressure pulsing. In cases of LNAPL contamination air would be expected to be in close proximity with the contaminant.

The LNAPL contaminant was an oil/varsol mixture with a viscosity similar to that found in a Southern Ontario field trial site. The varsol was needed to reduce the viscosity of the oil.

Figure E.1: Lab setup. The air has a slightly silver colour in this picture. Note the location of the inflow/outflow ports into the cell.

E.3 Procedure

The waterflood was initiated with a head of approximately 60cm. At the same time, pulsing was started using a rubber mallet to firmly compact the tubing leading to the cell entry (the CPS was not finished, see Appendix A). Pulsing was done at a frequency of approximately 1.5 pulses every second.

The experiment was discontinued when a visually significant amount of contaminant had been removed and water formed the majority of the outflow. Eight minutes had passed since the beginning of the test and approximately 700ml of water had been through the cell.

E.4 Results

The final and initial photos are shown in Figure E.2. The final matrix has compressed slightly, resulting in a narrow, empty area at the upper right. Pulsing was very effective at removing a large amount of contaminant quickly, however a quantitive estimate is not available. The results were impressive, considering the amount of air in the cell and expectations that more water would flow through the bottom layer. Although it is not visible in Figure E.2, the air is still present.

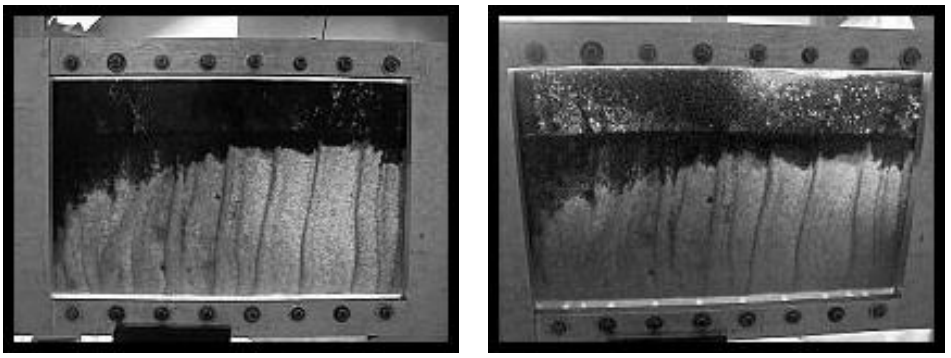

Original Final

Figure E.2: Initial and final photos. Taken with the same lighting, but unfortunately at slightly different angles.

Appendix F

Chemical Assisted, Pulsed Waterflood Tests

A suite of experiments was run to evaluate the effectiveness of standard oilfield solvents. Three different chemicals were used. However, because all chemicals produced similar results, only one result is shown here for simplicity. The experiments were done with 30–40 glass beads to ensure consistency. Crude, heavy oil was used as the reservoir fluid, and produced water as the displacing fluid. Produced water is the industry term for water produced from an oil well.

F.1 Lab Equipment

- digital camera and tripod
- electronic scale
- graduated cylinders
- experimental cell
- CPS (Consistent Pulsing Source)
- 30–40 glass beads
- produced water
- 3 different chemicals; 50 litres of water/chemical mixture for each chemical type
- crude heavy oil

F.2 Experimental Procedure and Setup

F.2.1 Water and Chemical Preparation

To ensure consistency, all produced water was mixed together first. The chemicals were mixed with produced water according to instructions provided by the chemical companies.

(a) To ensure that the produced water was consistent for all experiments, the water was siphoned into a large bucket and mixed.

(b) Interestingly, the produced water formed suds when mixed.

(c) The water was then poured into buckets for mixing with the chemical.

(d) The measured chemical being added to the produced water buckets.

(e) Siphoning the chemical into the CPS water reservoir

Figure F.1: The produced water and chemical preparation

F.2.2 Equipment Setup

1. Fill the experimental cell with water.

2. Weigh the medium and fill the cell with it (approximately 2.5 kg if using glass beads).
3. Set porosity by altering the volume of the cell (medium mass is known, medium density can be measured). Porosity was 35.5% for all experiments.
4. Flood the cell with produced crude oil overnight.

F.2.3 Pulsing procedure

1. Attach the cell to the Consistent Pulsing Source (CPS).
2. Place graduated cylinders at the outflow.
3. Run the experiment using standardized pulse pressure/period settings (one pulse every 0.75 seconds, 5.5 psi pulse amplitude).
4. Measure outflow oil/water concentrations as the test proceeds.
5. Stop the experiment after 1.5 pore volumes have been put through the system.

F.3 Results

The results are shown in Figure F.3. The final sweep efficiencies at one pore volume were 25%, 15%, 15%, and 8% for the pulsed chemical, non-pulsed chemical, pulsed water, and non-pulsed water, respectively. Pulsed tests were approximately 1 hour in duration, non-pulsed tests were about 6 hours for equivalent pore volumes.

F.4 Discussion and Conclusions

The oilfield solvent was shown to greatly increase sweep efficiency. This is because it reduced the oil/water interfacial tension, resulting in a more efficient sweep. It may be possible to give sweep efficiency estimates by measuring the oil/water interfacial tension.

Surprisingly, the non-pulsed chemical and pulsed water performed equally well with respect to pore volumes. However, it may not be a fair comparison because the head placed on the system was very small (0.75 m). The non-pulsed experiment lasted approximately 6 times as long, giving the chemical more time to react.

(a) Experimental cell half-filled with water

(b) Pouring 30–40 mesh glass beads into the cell

(c) Filled experimental cell with compression bracket

(d) Cell with heating pads being oil flooded (oil/water interface is visible above the duct tape). The reservoir was cooled to room temperature overnight.

Figure F.2: Setup steps for the chemical experiment.

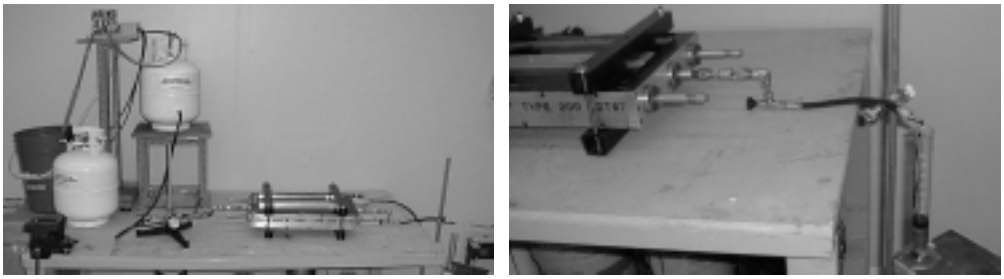

(a) Laboratory setup showing (from right to left) the experimental cell, water reservoir, solenoid valves, air ballast tank, and exhaust bucket (for collecting fluid blown out the exhaust).

(b) Experimental cell outflow and graduated cylinder

Figure F.3: The setup for the chemical experiments

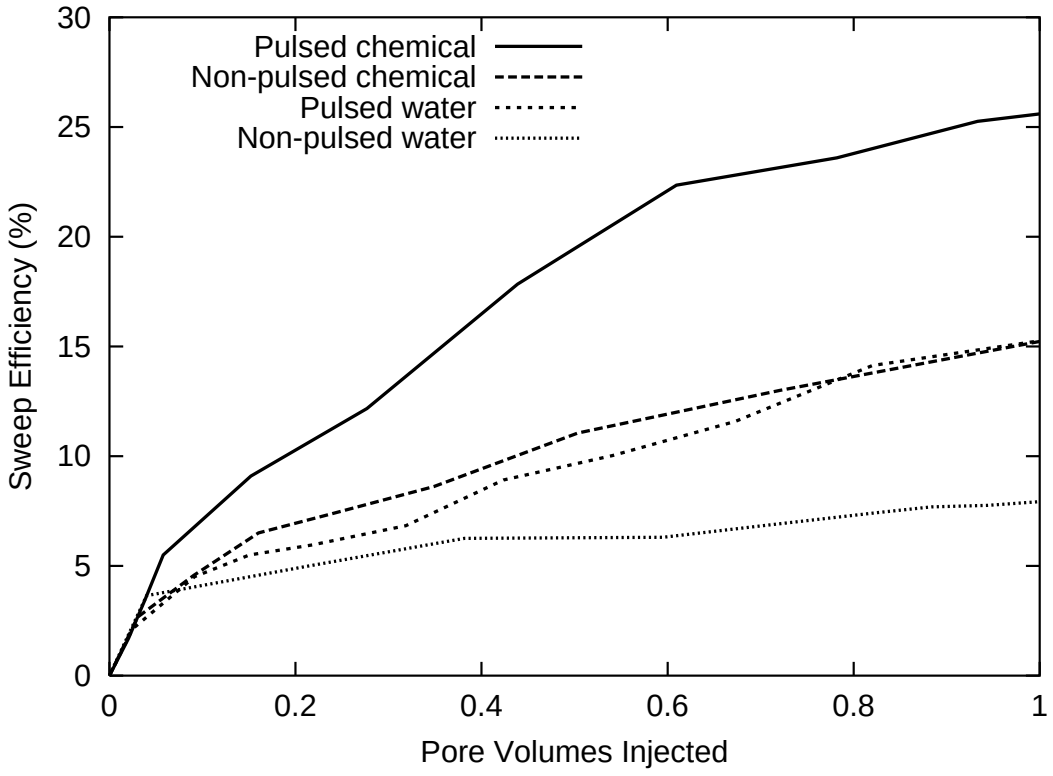

Figure F.4: Results of the chemical experiments